

## Article

# Understanding Rainfall Distribution Characteristics over the Vietnamese Mekong Delta: A Comparison between Coastal and Inland Localities

Huynh Vuong Thu Minh <sup>1</sup>, Bui Thi Bich Lien <sup>2</sup>, Dang Thi Hong Ngoc <sup>3</sup>, Tran Van Ty <sup>4</sup>, Nguyen Vo Chau Ngan <sup>1</sup>, Nguyen Phuoc Cong <sup>4</sup>, Nigel K. Downes <sup>1</sup>, Gowhar Meraj <sup>5</sup> and Pankaj Kumar <sup>6,\*</sup>

<sup>1</sup> Water Resources Department, College of Environment and Natural Resources, Can Tho University, Can Tho 900000, Vietnam

<sup>2</sup> Environment and Natural Resources Management Department, College of Environment and Natural Resources, Can Tho University, Can Tho 900000, Vietnam

<sup>3</sup> Faculty of Natural Resource and Environment, Kien Giang University, Kien Giang 920000, Vietnam; dthngoc@vnkgu.edu.vn

<sup>4</sup> Water Resource Engineering Department, College of Engineering, Can Tho University, Can Tho 900000, Vietnam

<sup>5</sup> Department of Ecosystem Studies, Graduate School of Agricultural and Life Sciences, The University of Tokyo, Tokyo 113-0032, Japan; gowharmeraj@g.ecc.u-tokyo.ac.jp

<sup>6</sup> Institute for Global Environmental Strategies, Hayama 240-0115, Japan

\* Correspondence: kumar@iges.or.jp

**Abstract:** This study examines the changing rainfall patterns in the Vietnamese Mekong Delta (VMD) utilizing observational data spanning from 1978 to 2022. We employ the Mann–Kendall test, the sequential Mann–Kendall test, and innovative trend analysis to investigate trends in annual, wet, and dry season rainfall, as well as daily rainfall events. Our results show significant spatial variations. Ca Mau, a coastal province, consistently showed higher mean annual and seasonal rainfall compared to the further inland stations of Can Tho and Moc Hoa. Interestingly, Ca Mau experienced a notable decrease in annual rainfall. Conversely, Can Tho, showed an overall decrease in some months of the wet season and an increase in dry season rainfall. Furthermore, Moc Hoa showed an increase in the number of rainy days, especially during the dry season. Principal component analysis (PCA) further revealed strong correlations between annual rainfall and extreme weather events, particularly for Ca Mau, emphasizing the complex interplay of geographic and climatic factors within the region. Our findings offer insights for policymakers and planners, thus aiding the development of targeted interventions to manage water resources and prepare for changing climate conditions.

**Keywords:** climate change; Vietnamese Mekong Delta (VMD); rainfall patterns; Mann–Kendall test; innovative trend analysis; principal component analysis; coastal and riverine ecosystems



**Citation:** Minh, H.V.T.; Lien, B.T.B.; Hong Ngoc, D.T.; Ty, T.V.; Ngan, N.V.C.; Cong, N.P.; Downes, N.K.; Meraj, G.; Kumar, P. Understanding Rainfall Distribution Characteristics over the Vietnamese Mekong Delta: A Comparison between Coastal and Inland Localities. *Atmosphere* **2024**, *15*, 217. <https://doi.org/10.3390/atmos15020217>

Academic Editor: Tomeu Rigo

Received: 28 December 2023

Revised: 4 February 2024

Accepted: 7 February 2024

Published: 10 February 2024



**Copyright:** © 2024 by the authors. Licensee MDPI, Basel, Switzerland. This article is an open access article distributed under the terms and conditions of the Creative Commons Attribution (CC BY) license (<https://creativecommons.org/licenses/by/4.0/>).

## 1. Introduction

Southeast Asia consists of 11 countries, most of which are archipelagos [1,2]. The complicated distribution of land, sea, and topography causes the climate to change dramatically across time and place [1,2]. According to various studies [3,4], heatwaves have increased in recent decades, accompanied by weakened monsoon seasons, resulting in less rainfall and hotter weather. Vietnam is situated on the east coast of the Indochina Peninsula. It is divided from the rest of the peninsula by the Truong Son Mountain Range, also known as the Annamite Range, which runs parallel to the coast [5,6]. Vietnam has a characteristic monsoon-influenced climate like that of mainland Southeast Asia. The wide range of topography, long span of latitude (Vietnam spans over 15° of latitude), and influences from the East Sea result in climatic conditions that differ between regions. The climate is additionally impacted by the El Niño Southern Oscillation, which shapes monsoonal

circulation and prompts intricate changes in rainfall and temperature patterns that differ spatially at a subnational level [7–9]. Many studies also suggest that tropical cyclones affect rainfall patterns in Vietnam. According to Garcia, Vietnam is struck by an average of four to six typhoons per year [10]. The central region of Vietnam experiences more tropical cyclones than other regions, peaking in October and November. The maximum number of tropical cyclones occurs in the northern region from July to September, while nontropical cyclones account for most of the total rainfall in the southern region [11].

Vietnam has been classified by the Intergovernmental Panel on Climate Change as one of the country's most likely to be impacted by climate change due to its extensive coastline, vast agriculturally significant river deltas and floodplains, location on the path of typhoons, and large impoverished populations that are dependent on climate-sensitive economies [12–14]. Changes in rainfall patterns are significant for socioeconomic development planning and national security, in particular for forecasting the onset of droughts and flood events, as well as assessing surface and groundwater water resources and their quality [15]. Many studies have highlighted the regional variations in rainfall patterns, notably decreases in the north of Vietnam and increases volumes in the south [16]. The distribution and length of the rainy season and the number of rainy days has also changed.

The Vietnamese Mekong Delta (VMD) is a low-lying freshwater ecosystem, a hotspot of biodiversity and an agricultural production zone that contributes to the lives and livelihoods of more than 21 million people. The VMD offers the basis for inclusive socioeconomic development that can help eradicate poverty throughout the region. However, the VMD is additionally one of the regions of the world that is most affected by climate change. Those residing in this delta are particularly exposed to natural hazards that are caused or exacerbated by climate change. The number and intensity of climate-induced disasters, such as floods and droughts, are already increasing noticeably. In the VMD, 5% of the water comes from rainfall. The influence of geography and local natural conditions has affected the spatial distribution of rainfall, particularly the differences between rainfall variation in coastal areas and inland areas. Climate change is making weather events more extreme, not only by altering the mean and variability, making wet seasons wetter and dry seasons drier, but also through the spatial distribution of rainfall [17,18]. Currently, little understood about how the characteristics of rainfall vary from coastal to inland areas or how these changes relate to certain largescale oscillations [18].

To evaluate recent climate change trends, non-parameter tests were conducted. Firstly, we applied the Mann–Kendall statistical test to detect monotonic trends in data. A large bevy of previous studies have used this statistical test to ascertain the presence of statistically significant trends in meteorological and climatic timeseries datasets [18–23]. Furthermore, Sen's slope estimator can yield a trend slope estimate and is comparatively robust to outliers. Although this test is extensively used for trend detection, it has several problems related to serial correlation in timeseries data. To address this issue, modified Mann–Kendall (MMK) and the trend-free pre-whitening Mann–Kendall (TFPW-MK) tests have been created. These tests yield more accurate results than the MK test, but they are also heavily dependent on sample size and data distribution. As a result, innovative trend analysis (ITA) was established to address the shortcomings of the MK test [24,25]. Prior studies have reported that ITA provides reliable results over the MK test to detect trends in climate parameters [19,26–28]. Furthermore, as of late, innovation trend analysis (ITA) has gained popularity [24], as it is capable of capturing nonlinear trends and offers additional insights into the data's structure, including trend identification across all value ranges [29]. Serinaldi et al. recently reported that sample size and data dispersion also affect ITA [30]. Thus, it is crucial to investigate rainfall trends using nonparametric methods other than the ITA method in order to better understand rainfall variability by comparing the results to those obtained using other methodologies [25].

We selected three distinct areas of the VMD to analyze changes in rainfall characteristics over time and under climate change conditions. (i) Ca Mau is a coastal plain province of the VMD. The climate in Ca Mau, in recent years, has not been as distinctly divided

as before, with the rainy season is no longer concentrated from May to November and the dry season months no longer occurring from December to April of the following year. Now, rain is often observed scattered throughout all months of the year. Ca Mau has a very unique climate, with periods of wetness and dryness occurring in the same year [8]. (ii) Can Tho city is located in the mid-lower region of the VMD, while (iii) Moc Hoa is located in the tropical monsoon and hot and humid climate zone. Because of the contiguity between the two regions of the Southeast and the Mekong Delta, this area not only has the typical characteristics of the Mekong Delta but also has the unique characteristics of the Southeast region. The issue of climate change has become a critical concern for the sustainable development of the VMD [25]. As spatial and temporal rainfall characteristics are an important part of the hydrologic cycle, their examination will aid the improved understanding of flood, drought, saline water intrusion, and extreme weather [28,31–33]. The goal of this study is to evaluate how climate change affects the distribution of spatiotemporal rainfall in the three different areas of the VMD. The results can inform the scientific basis for local managers to draft and plan appropriate adaptation strategies for future changes in rainfall distributions.

## 2. Materials and Methods

### 2.1. Study Area

Datasets from the three meteorological stations were used to assess the changes in rainfall characteristics along the transect from the coastal to inland regions of the VMD (Figure 1). The first selected meteorological station is located in Ca Mau, Vietnam's and the VMD's most southern province. This coastal province is a peninsula encompassed by the sea on three sides and incised by a dense network of rivers and canals. In total, the province has a coastline of over 250 km. The second meteorological station we assessed is Can Tho station in Can Tho City. Can Tho is located in the middle and lower reaches of the VMD. The province stretches for over 55 km along the west bank of the Hau River, with a total natural land area of 1401.61 km<sup>2</sup>. The third station selected was Moc Hoa in Long An province. Long An is located in the transitional zone between Vietnam's southeast and southwest regions. Therefore, Moc Hoa not only exhibits the typical climatic characteristics of the VMD, but also the unique characteristics of the southeast region.

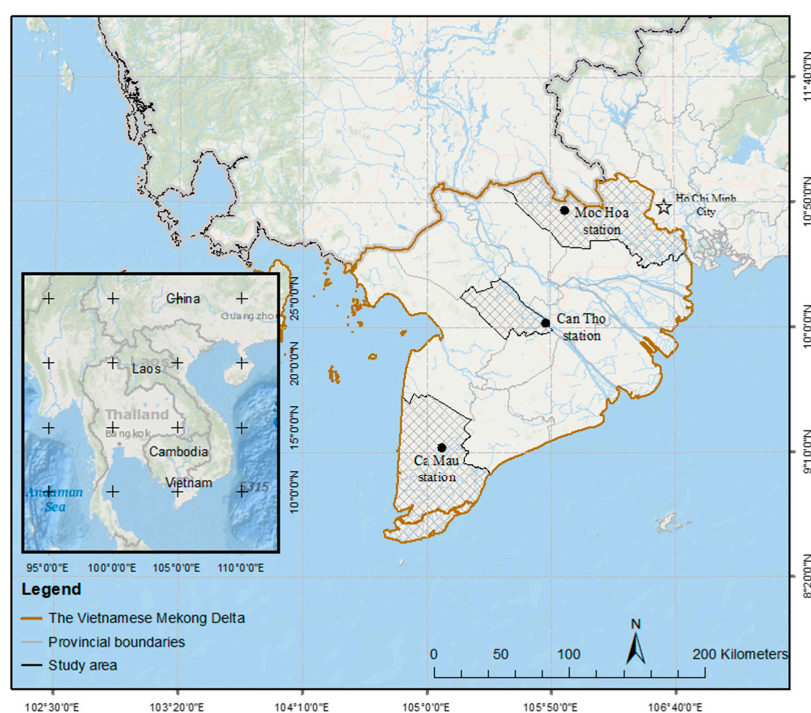


**Figure 1.** Location of three studied meteorological stations in the VMD.

Data collection: Daily rainfall data for the 45-year period from 1978 to 2022 was recorded at the three meteorological stations.

### 2.2. Rainfall Correlation Matrix and Principal Component Analysis

A Pearson matrix correlation analysis was conducted to examine the rainfall characteristics that influence the annual wet season and dry season rainfall volumes and distributions. We used an accuracy index with the Pearson correlation coefficient as shown in Equation (1):

$$R = \frac{n\sum_{i=1}^j (x_i y_i) - (\sum_{i=1}^j x_i)(\sum_{i=1}^j y_i)}{\sqrt{\left[ n(\sum_{i=1}^j (x_i^2)) + (\sum_{i=1}^j x_i)^2 \right] \left[ n(\sum_{i=1}^j (y_i^2)) + (\sum_{i=1}^j y_i)^2 \right]}} \tag{1}$$

The Evans standard (1996) [34] was adopted to determine the level of Pearson correlation matrix strengths (Table 1). Here, the R values vary from −1 to 1, with positive values indicating a positive correlation (two variables increase or drop together) and negative values indicating a negative correlation (one variable increases while the other decreases).

**Table 1.** Strengths of the Pearson correlation matrix.

Level of Statistical Strength	Pearson Correlation Matrix (R)
Very strong	0.80–1.00
Strong	0.60–0.79
Moderate	0.40–0.59
Weak	0.20–0.39
Very weak	0.00–0.19

The CA tool was applied to examine the data for spatial and temporal differences, which previous research has applied to hydrological and meteorological data [35–37]. The PCA was used to transform the original variables into new principal components performed along directions of maximum variance. Also, reducing the contribution of less significant variables with minimal information loss was identified. In this study, the principal component was applied to identify which factors will be the most important parameters of water quality, as expressed in Equation (2) (see references [38–40]):

$$Z_{ij} = a_{1i}x_{1j} + a_{2i}x_{2j} + \dots + a_{im}x_{mj} \tag{2}$$

where Z is the component score, a is component loading, x is component number, j is sample number, and m is a total number of variables.

### 2.3. Rainfall Trend Analysis

Because the rainfall data at the stations did not follow a normal distribution, non-parametric tests were employed in this study. We conducted the Mann–Kendall test, the sequential Mann–Kendall test, and innovative trend analysis, which have been used extensively in a number of past studies [23,41–44]. The Mann–Kendall statistic determines the presence of a trend and whether that trend is positive or negative based on the range of Mann–Kendall statistics (between −1 and 1). The positive values of the test statistics (S) indicate an increasing trend, whereas negative values suggest a falling trend. The Mann–Kendall equation, which is based on the S statistic (Equation (3)) [45,46], is as follows:

$$S = \sum_{j=1}^{n-1} \sum_{i=j+1}^n \text{sign}(x_i - x_j) \tag{3}$$

where,  $x_i$  and  $x_j$  are sequential data values in timeseries  $i, j$ ,  $n$  is the length of time series, and  $sign(x_i - x_j)$  is the sign function as shown in Equation (4):

$$Sign(x_i - x_j) = \begin{cases} +1 & \text{if } (x_i - x_j) > 0 \\ 0 & \text{if } (x_i - x_j) = 0 \\ -1 & \text{if } (x_i - x_j) < 0 \end{cases} \tag{4}$$

The variance is computed as shown in Equation (5):

$$Var(S) = \frac{1}{18} \left[ \sum_{p=1}^g t_p(t_p - 1)(2t_p + 5) - \frac{n(n-1)(2n+5)}{2} \right] \tag{5}$$

where  $n$  is the number of data points,  $g$  is the number of tied groups, and  $t_p$  denotes the number of data values in the  $p$  th group. If there are no tied groups, this summary process can be ignored [44]. A tied group is a set of sample data having the same value. In cases where the sample size  $n > 30$ , the standard normal test statistic  $Z_s$  is computed using Equation (6) [23]:

$$Z_s = \begin{cases} \frac{S - 1}{\sqrt{Var(S)}} & S > 0 \\ 0 & S = 0 \\ \frac{S + 1}{\sqrt{Var(S)}} & S < 0 \end{cases} \tag{6}$$

Positive values of  $Z_s$  indicate increasing trends, while negative  $Z_s$  values show decreasing trends. Testing trends is performed at the specific  $\alpha$  significance level. When  $|Z_s| > Z_{1-\alpha/2}$ , the null hypothesis is rejected, and a significant trend exists in the timeseries.  $Z_{1-\alpha/2}$  is obtained using the standard normal distribution table. In this study, significance levels  $\alpha = 0.01$  and  $\alpha = 0.05$  were used. At the 5% significance level, the null hypothesis of no trend is rejected if  $|Z_s| > 1.96$ . It is also rejected if  $|Z_s| > 2.576$  at the 1% significance level.

Sen’s slope estimator (Sen 1968) [47] can be used to estimate the slope or rate of change in hydrometeorological timeseries. The slopes of each pair of data are computed to provide an estimate of the slope  $Q$ , as shown in Equation (7):

$$Q_i = \frac{X_j - X_k}{j - k} \quad \text{for } i = 1, \dots, n \tag{7}$$

where  $X_j$  and  $X_k$  are the data values at times  $j$  and  $k$  ( $j > k$ ), respectively. If there is only one datum in each time period, then  $N = \frac{n(n-1)}{2}$ , where  $n$  is the number of time periods. If there are multiple observations in one or more time periods, then  $N < \frac{n(n-1)}{2}$ . The  $n$  values of  $Q_i$  are ranked from smallest to largest, and the median of slope or Sen’s slope estimator is computed as shown in Equation (8):

$$Q_{med} = \begin{cases} Q_{(n+1)/2} & N \text{ is odd} \\ \frac{Q_{n/2} + Q_{(n+2)/2}}{2} & N \text{ is even} \end{cases} \tag{8}$$

The  $Q_{med}$  sign reflects a data trend, while its value indicates the steepness of the trend. To determine whether the median slope is statistically different than zero, one should obtain the confidence interval of  $Q_{med}$  at a specific probability. The confidence interval of the time slope [48] can be computed as show in Equation (9):

$$C_\alpha = Z_{1-\alpha/2} \sqrt{Var(S)} \tag{9}$$

The S-MK test is used to determine if the series is increasing or decreasing with time. While the test displays the data graphically, it also determines the trend’s starting point [49]. The  $t$  value denotes the test statistic, which was calculated by summing the

$n_i$  values obtained by counting the smaller ones from the previous ranks for each rank (Equation (10)).

$$t = \sum_{i=1}^n n_i \quad (10)$$

The mean value, variance  $Var(t)$ , and test statistic  $u(t)$  were calculated as shown in Equations (11), (12), and (13), respectively. The backward test statistic  $u'(t)$  is calculated similarly to  $u(t)$ .

$$E(t) = \frac{n(n-1)}{4} \quad (11)$$

$$Var(t) = \frac{n(n-1)(2n+5)}{72} \quad (12)$$

$$u(t) = \frac{(t - E(t))}{\sqrt{Var(t)}} \quad (13)$$

Innovative trend analysis (ITA) was developed by Sen (2012) [24,50]. ITA has shown some benefits over the Mann–Kendall test, which have been illustrated via a comparison of the two approaches [51]. The timeseries is separated into two similar groups, each of which is classified in ascending order. Following that, both the first and second parts of the timeseries are plotted on the X and Y axes, respectively. If the data are collected on the 1:1 ideal line (45° line), the timeseries exhibits no trend. When data are placed on the upward triangular edge of the ideal line, the timeseries continues to grow. When data are aggregated in the downward triangular region of the 1:1 line, the timeseries shows a falling trend [24,50]. If the scatter points do not correspond to growing or decreasing trends, the data is then divided into “low”, “medium”, and “high” value groups [52]. Thus, this method allows for the obvious identification of low-, medium-, and high-value trends in any climate timeseries [24,26,51]. The “low”, “medium”, and “high” value groups were based on the percentiles [53] according to the low ( $X < \bar{X} - S_x$ ), medium ( $\bar{X} - S_x < X < \bar{X} + S_x$ ), and high levels ( $X > \bar{X} + S_x$ ).  $\bar{X}$  denotes mean value, and  $S_x$  denotes standard deviation.

### 3. Results

#### 3.1. Descriptive Statistics

In general, the results highlight different annual rainfall distribution volumes for all three assessed stations. Total annual rainfall decreased from the coastal to the inland stations along the transect (Table 2). The mean annual rainfall over the assessment period in Ca Mau, Can Tho, and Moc Hoa was 2360 mm, 1624 mm, and 1595 mm, respectively. The mean annual rainfall in Ca Mau was approximately 31% and 32% higher than that of Can Tho and Moc Hoa, respectively. Similarly, Ca Mau exhibited 30% and 32% more rainfall during the wet season than both Can Tho and Moc Hoa. It should be noted that, the mean rainfall in Ca Mau during the dry season was also approximately 43% and 33% higher than in Can Tho and Moc Hoa. Can Tho also recorded the lowest rainfall of all three stations during the dry season. The maximum daily rainfall and number of days with rainfall exceeding 50 mm were also higher in Moc Hoa than in Can Tho. The observed decrease in total annual rainfall from coastal to inland stations suggests a gradient influenced by geographical factors and, potentially, by monsoonal patterns [54]. Hence, due to the direct exposure to monsoon winds, coastal areas like Ca Mau typically receive more rainfall, while inland areas, such as Moc Hoa, receive less [55].

**Table 2.** Summary statistics of rainfall during the period from 1978 to 2022 for the three meteorological stations.

Variable	Observations	Minimum	Maximum	Mean	Std. Deviation	Coefficient of Variation
Ca Mau station						
Annual rainfall (mm)	45	1743	3580	2360	350	0.15
Wet season rainfall (mm)	45	1610	2741	2127	290	0.14
Dry season rainfall (mm)	45	26	930	233	152	0.65
Daily maximum rainfall (mm)	45	61	189	111	31	0.28
Daily rainfall exceeding 50 mm (day)	45	3	14	9	2	0.28
No. rainfall days (day)	45	144	213	171	13	0.08
No. wet season rainfall days (day)	45	131	163	145	8	0.05
No. dry season rainfall days (day)	45	9	66	26	11	0.43
Can Tho station						
Annual rainfall (mm)	45	1160	2431	1624	260	0.16
Wet season rainfall (mm)	45	948	2009	1492	236	0.16
Dry season rainfall (mm)	45	20	424	132	98	0.74
Daily maximum rainfall (mm)	45	48	165	88	23	0.26
Daily rainfall exceeding 50 mm (day)	45	0	12	4	2	0.53
No. rainfall days (day)	45	119	185	154	13	0.09
No. wet season rainfall days (day)	45	114	163	137	10	0.07
No. dry season rainfall days (day)	45	5	44	17	8	0.51
Moc Hoa station						
Annual rainfall (mm)	45	1047	2433	1595	323	0.20
Wet season rainfall (mm)	45	963	2142	1440	309	0.21
Dry season rainfall (mm)	45	15	371	154	91	0.59
Daily maximum rainfall (mm)	45	54	240	99	37	0.37
Daily rainfall exceeding 50 mm (day)	45	1	10	5	2	0.47
No. rainfall days (day)	45	113	177	144	14	0.09
No. wet season rainfall days (day)	45	101	149	126	10	0.08
No. dry season rainfall days (day)	45	4	48	18	9	0.47

### 3.2. Correlation and Principal Component Analysis (PCA) for Examining Rainfall Characteristics

Table 3 demonstrates that the annual rainfall volumes in Ca Mau had a very strong Spearman correlation with wet season rainfall, at 0.936, strong correlation with daily rainfall above 50 mm, at 0.64, and a moderate correlation with daily maximum rainfall, at 0.533. The wet season rainfall also showed a strong correlation with daily rainfall above 50 mm and maximum daily rainfall ( $r = 0.611$ ) and moderate correlation with daily maximum rainfall ( $r = 0.594$ ); however, the dry season rainfall has a strong correlation with dry season rainfall days and moderate correlation with the overall number of rainy days. In general, annual rainfall and wet season rainfall were heavily influenced by the number of daily rainfalls above 50 mm. Therefore, there are significant differences in rainfall between the wet and dry seasons across all stations, which is a characteristic feature of monsoon climates. More specifically, monsoon's influence is evident in the substantial increase in rainfall during the wet season, which is a direct result of the southwest monsoon that affects the region from May to October [55,56]. However, rainfall during the dry season was most affected by the number of dry season days. These results indicate that the PCA results would provide more details related to the rainfall characteristics in Ca Mau.

Based on a diverse range of rainfall features in Ca Mau, Figure 2 displays the PCA results that separated the annual rainfall datasets into four major categories. Groups I and II experienced higher annual rainfall than the other categories. Group I often experienced substantial annual rainfall volumes in certain years as a result of La Niña. The La Niña years include 1989, 1995, 1996, 1999, 2000, 2006, 2008, 2011, and 2022 [57]. Group II is especially notable because it includes years in which one year is afflicted by both El Niño during the dry season and La Niña during the wet season. This group is characterized by very high rainfall during the wet season and very low rainfall during the dry season. Consequently, Group II still exhibited high rainfall volumes, although they are less than those of Group I. Group III includes the years with the least amount of annual rainfall relative to the other groups. It is significant to note that the amount of rainfall in Group III

was most impacted by El Niño in all years with low rainfall. The years when El Niño was pronounced are 1983, 1987, 1991, 2004, 2010, 2014, 2016, and 2019 [58]. Consequently, the total annual rainfall volume is minimal because both wet and dry season rainfall volumes were low. In addition, other rainfall characteristics are low in Group III (Figure 2). Group IV shows higher rainfall figures than Group III because the years in this group had a high dry season rainfall, despite low wet season rainfall. Additionally, Figure 2 shows that, although the number of rainy days varied little, wet season rainfall, annual rainfall, daily rainfall exceeding 50 mm, and maximum daily rainfall all varied significantly in Ca Mau. These results highlight the monsoon’s sensitivity to broader climatic oscillations [59]. El Niño typically weakens the monsoon, leading to drier conditions, while La Niña strengthens it, resulting in more rainfall [60]. Moreover, as certain years with higher rainfall volumes are often associated with La Niña events, this further emphasizes the monsoon’s role in regional rainfall variability [61].

**Table 3.** Correlation matrix showing Spearman correlation analysis between rainfall characteristics in Ca Mau station.

Variables	Var 1	Var 2	Var 3	Var 4	Var 5	Var 6	Var 7	Var 8
Annual rainfall (Var 1)	<b>1</b>							
Wet season rainfall (Var 2)	<b>0.936</b>	<b>1</b>						
Dry season rainfall (Var 3)	<b>0.315</b>	−0.009	<b>1</b>					
Daily maximum rainfall (Var 4)	<b>0.533</b>	<b>0.594</b>	−0.076	<b>1</b>				
Daily rainfall exceeding 50 mm (day) (Var 5)	<b>0.640</b>	<b>0.611</b>	0.228	<b>0.300</b>	<b>1</b>			
No. rainfall days (Var 6)	<b>0.323</b>	0.150	<b>0.562</b>	−0.039	0.081	<b>1</b>		
No. wet season rainfall days (Var 7)	<b>0.299</b>	<b>0.313</b>	0.046	0.141	0.114	<b>0.628</b>	<b>1</b>	
No. dry season rainfall days (Var 8)	0.262	0.012	<b>0.740</b>	−0.122	0.102	<b>0.677</b>	−0.087	<b>1</b>

Values in bold are different from 0, with a significance level of alpha = 0.05.

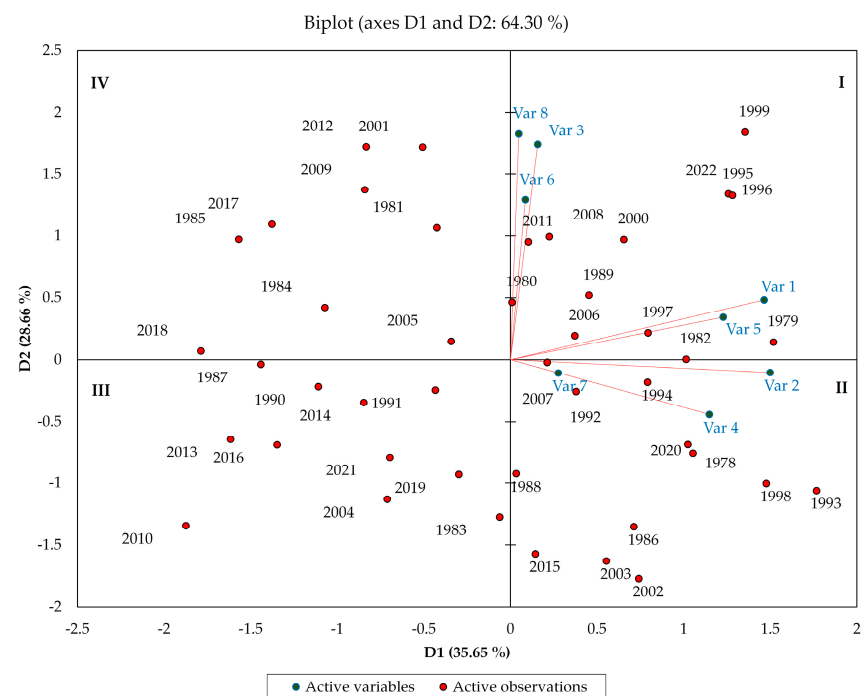


**Figure 2.** Contribution of the variables and observation of rainfall at Ca Mau station.

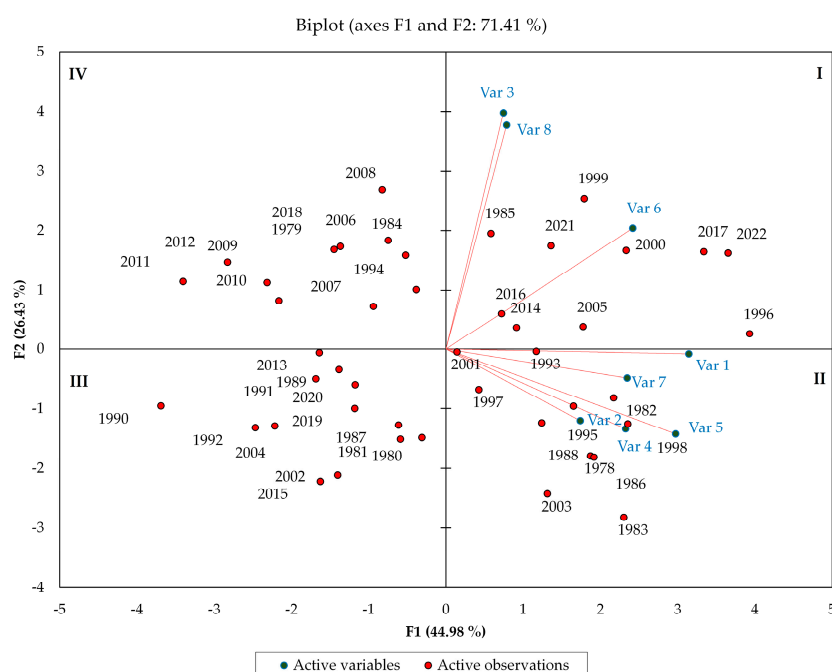
Table 4 and Figure 3 demonstrate that the annual rainfall in Can Tho station (Var 1) was very strongly correlated to wet season rainfall, with a correlation coefficient of 0.923; strongly correlated to daily rainfall over 50 mm ( $r = 0.678$ ); moderately correlated to the

number of rainfall days and the number of wet season rainfall days (with correlation coefficient of 0.590 and 0.554, respectively).

**Table 4.** Correlation matrix showing Spearman correlation analysis between rainfall characteristics in Can Tho station.

Variables	Var 1	Var 2	Var 3	Var 4	Var 5	Var 6	Var 7	Var 8
Annual rainfall (Var 1)	<b>1</b>							
Wet season rainfall (Var 2)	<b>0.923</b>	<b>1</b>						
Dry season rainfall (Var 3)	0.258	−0.068	<b>1</b>					
Daily maximum rainfall (Var 4)	<b>0.448</b>	<b>0.460</b>	0.060	<b>1</b>				
Daily rainfall exceeding 50 mm (day) (Var 5)	<b>0.678</b>	<b>0.751</b>	−0.042	<b>0.395</b>	<b>1</b>			
No. of rainfall days (Var 6)	<b>0.590</b>	<b>0.424</b>	<b>0.422</b>	0.117	0.210	<b>1</b>		
No. wet season rainfall days (Var 7)	<b>0.554</b>	<b>0.578</b>	−0.085	0.247	0.225	<b>0.745</b>	<b>1</b>	
No. dry season rainfall days (Var 8)	0.193	−0.070	<b>0.813</b>	−0.116	−0.013	<b>0.534</b>	−0.069	<b>1</b>

Values in bold are different from 0, with a significance level of alpha = 0.05.



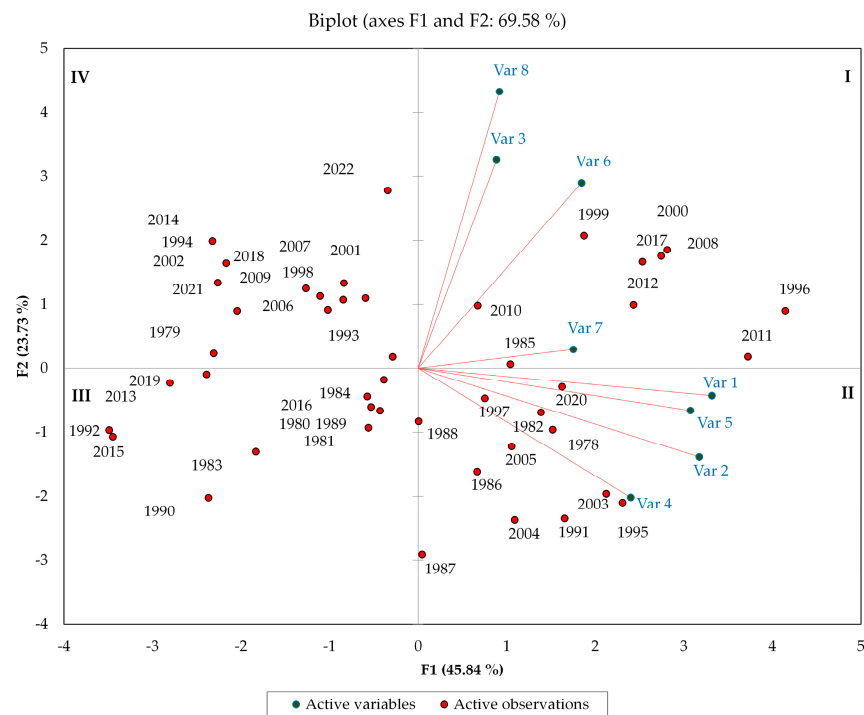
36% were affected by both neutral and El Niño, and 27% were mixed (either affected by El Niño, La Niña) and 10% of the high rainfall occurred during La Niña years. However, Group II received the second highest annual rainfall after Group I (1758 mm). Groups III and IV received the same amount of annual rainfall and were smaller than Groups I and II, containing fewer years. Groups III (1464 mm) and IV (1421 mm) account for less than 50% of all El Niño years. Within the framework of this investigation, we can see that the El Niño—Southern Oscillation (ENSO) had a smaller impact on rainfall at Can Tho station than it did at Ca Mau. It should be noted that all variables of rainfall characteristics were found to fluctuate over the years.

Table 5 and Figure 4 emphasize that the annual rainfall in Moc Hoa station (Var 1) has very strong correlation with wet season rainfall ( $r = 0.938$ ) and daily rainfall exceeding 50 mm ( $r = 0.896$ ) and a strong correlation with daily maximum rainfall ( $r = 0.638$ ). Wet season rainfall (Var 2) has a correlation with daily rainfall exceeding 50 mm ( $r = 0.826$ ) and the daily maximum rainfall ( $r = 0.624$ ). As expected, dry season rainfall has a correlation with the number of dry season rainfall days at 0.631 (strong).

**Table 5.** Correlation matrix showing Spearman correlation analysis between rainfall characteristics in Moc Hoa station.

Variables	Var 1	Var 2	Var 3	Var 4	Var 5	Var 6	Var 7	Var 8
Annual rainfall (Var 1)	<b>1</b>							
Wet season rainfall (Var 2)	<b>0.938</b>	<b>1</b>						
Dry season rainfall (Var 3)	0.289	−0.023	<b>1</b>					
Daily maximum rainfall (Var 4)	<b>0.638</b>	<b>0.624</b>	0.018	<b>1</b>				
Daily rainfall exceeding 50 mm (day) (Var 5)	<b>0.896</b>	<b>0.826</b>	0.271	<b>0.632</b>	<b>1</b>			
No. of rainfall days (Var 6)	<b>0.330</b>	<b>0.322</b>	0.193	0.066	0.196	<b>1</b>		
No. of wet season rainfall days (Var 7)	<b>0.313</b>	<b>0.428</b>	−0.193	0.198	0.193	<b>0.753</b>	<b>1</b>	
No. of dry season rainfall days (Var 8)	0.187	−0.006	<b>0.631</b>	−0.131	0.164	<b>0.603</b>	−0.008	<b>1</b>

Values in bold are different from 0, with a significance level of  $\alpha = 0.05$ .



**Figure 4.** Contribution of the variables and observation of rainfall at Moc Hoa station.

Rainfall in the three regions with similar points depends primarily on the daily rainfall exceeding 50 mm. The second element influencing rainfall at Ca Mau and Moc Hoa is the daily maximum rainfall, whereas Can Tho station is affected by the number of rainfall days.

Group I comprises all years with La Niña, and thus showed the most rainfall (average annual rainfall 2000 mm). Except for daily maximum rainfall, all rainfall variables were higher than those of the other groups. Group II showed the highest daily rainfall at 126 mm/day, whereas Group I had 115 mm/day. Overall, 92% of the years in Group II coincided with El Niño years, although the group exhibited the second highest average rainfall after Group I. Group III had the lowest rainfall, with 47%, 36%, and 18% for El Niño years, normal years, and La Niña years (1316 mm), respectively. Group IV is split 50/50 between El Niño and La Niña years.

Annual rainfall and rainfall during the wet season varied greatly over three locations. The number of wet season rainfall days at Ca Mau station, which is located in the coastal region, varied slightly. Furthermore, El Niño and La Niña have a greater influence on rainfall in coastal areas than inland localities. Furthermore, rainfall in Can Tho showed strong fluctuations in the number of rainy days.

### 3.3. Rainfall Trend Test

Figure 5 shows that the mean cumulative rainfall at all three study stations decreased during the period from 2000 to 2022 when compared with the period from 1978 to 2001. The mean cumulative rainfall in Ca Mau, Can Tho, and Moc Hoa fell by 14%, 4%, and 5%, respectively. Whereas, for Can Tho station, we observed that rainfall increased during the dry season. It should be noted that rainfall at Ca Mau station decreased in both the rainy and dry seasons. At Moc Hoa station, rainfall during the rainy season was seen to decrease, while it increased slightly during the dry season.

To investigate the rainfall characteristics, we conducted the Mann–Kendall trend test, the sequential Mann–Kendall test, and innovative trend analysis to better understand rainfall trends, including (i) the rainfall amount in each of the following seasons: annual, wet season, dry season, and the monthly (ii) daily maximum rainfall, daily rainfall exceeding 50 mm, and (iii) the number of days with rainfall (annually, wet and dry seasons). We also discovered that only the annual rainfall and wet season rainfall in Ca Mau had declined significantly at the 95% and 90% confidence level, respectively, using the Mann–Kendall test (Figure A1). August rainfall and Jun rainfall also had declined significantly at the 95% and 90% confidence level, respectively. The results of Sen's Slope calculation show the rate of decrease in annual rainfall, wet season rainfall, August rainfall, and Jun rainfall were found to be 8.25 mm/year, 6.8 mm/year, 3.2 mm/year, and 2.5 mm/year, respectively. However, the dry season rainfall and number of dry season rainfall day in Can Tho increased significantly at the 95% and 90% confidence level, respectively (Figure A2). The results of Sen's Slope calculation show the rate of increase in dry season rainfall and number of dry season rainfall days were 2.7 mm/year and 18 day/decade, respectively. In Can Tho station, we also found the increased significantly in August rainfall and Jun rainfall at the 95% and 90% confidence level, respectively. The results of Sen's Slope calculation show the rate of decrease in August rainfall and Jun rainfall were 1.8 mm/year and 1.77 mm/year. In Moc Hoa station, we found the number of rainfall days and the number of dry season rainfall days in Moc Hoa had increased significantly at the 95% and 90% confidence level, respectively (Figure A3). The results of Sen's Slope calculation show the rate of increase in the number of rainfall days and the number of dry season rainfall days were 3.2 day/decade and 2.5 day/decade, respectively.

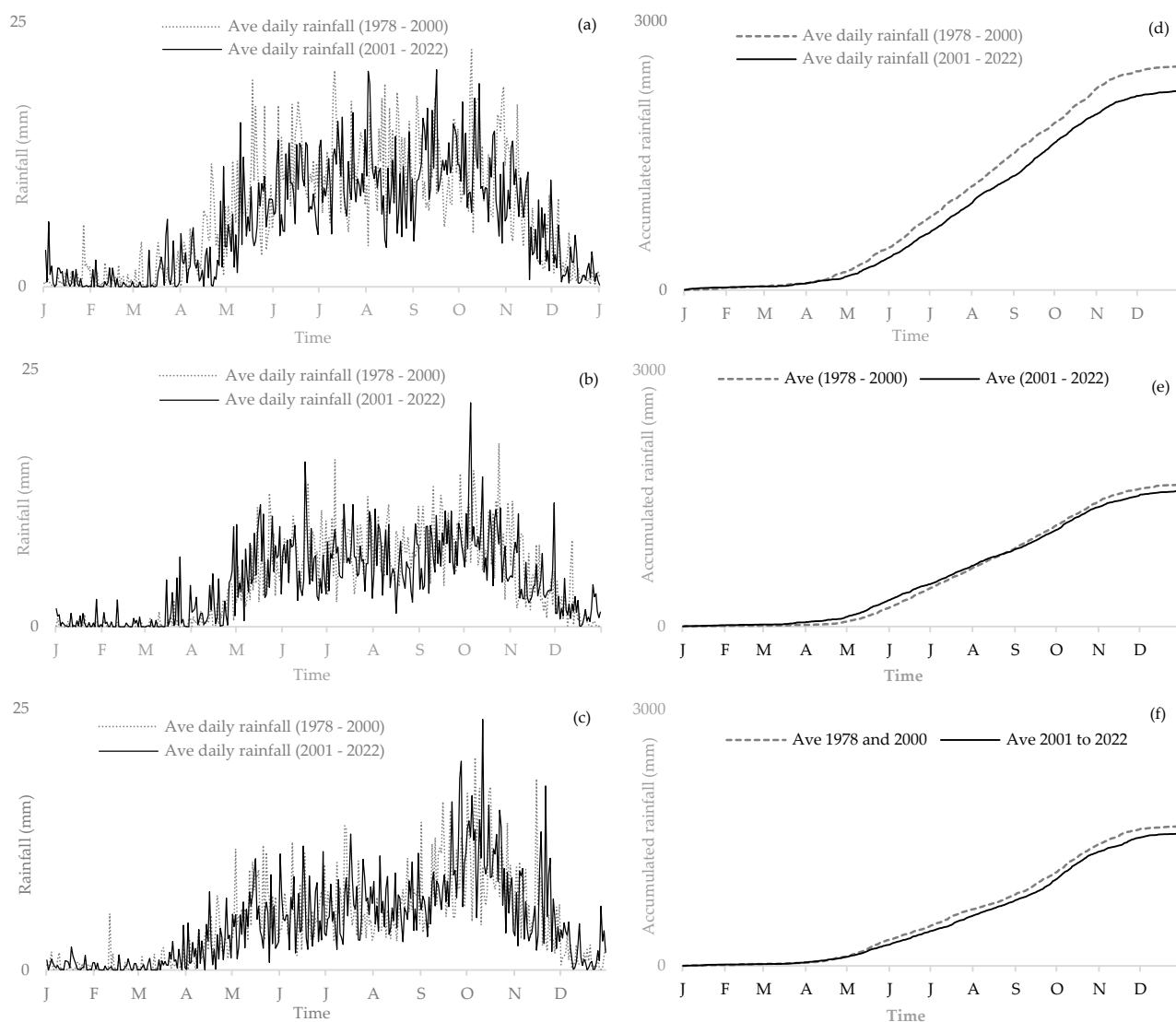


**Figure 5.** The comparison of daily rainfall and accumulated rainfall during the periods from 1978 to 2000 and 2011 to 2022 for Ca Mau (a,d), Can Tho (b,e), and Moc Hoa (c,f).

Figure 6 displays the trends of rainfall characteristics for the three assessed meteorological stations at a 95% confidence level using S-MK and ITA.

Between 1978 and 2022, the amount of annual rainfall in Ca Mau significantly decreased by 95% (Figure 6a). We discovered that the amount of annual rainfall overall has declined since 2007, with this decline being statistically significant since 2016. Innovative trend analysis classified this decrease in annual rainfall as “low” to “medium” level because most of the points plot is below the 1:1 line and based on the percentiles. The annual rainfall volumes in both the rainy and dry seasons decreased between 1978 and 2022. The annual rainfall volumes fell more during the wet season than during the dry season. This drop in rainfall during the wet season was statistically significant at 90%, whereas the drop during the dry season was not statistically significant. The annual rainfall at Can Tho station varied from year to year, with no discernible trend. We noticed that the overall wet season rainfall volume decreased during 1978–2022, but this is not statistically significant. Meanwhile, dry season rainfall volumes increased at the 95% confidence level over 45 years. The drop in wet season rainfall was because of a decrease in the number of rainy days during the wet season, and the increase in dry season rainfall was likewise because of an increase in the number of rainy days during the dry season. According to ITA results, the drop in

wet season rainfall from 1978 to 2022 varies from “medium” to “high” levels, whereas the increase in dry season rainfall was at the “medium” level.

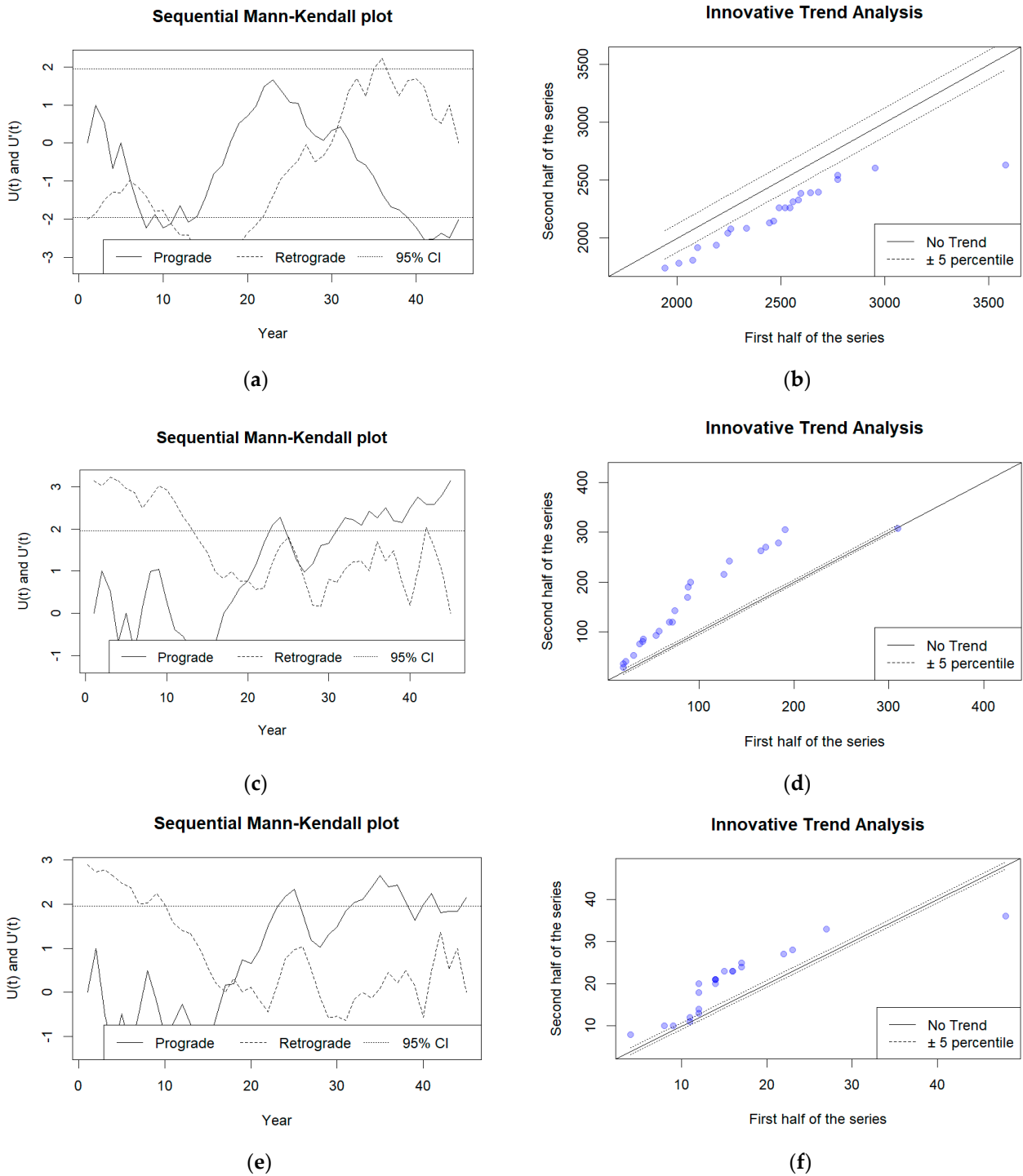


**Figure 6.** Rainfall trend patterns: (a) Annual rainfall decreasing trend in Ca Mau using S-MK. (b) Annual rainfall decreasing trend in Ca Mau using ITA. (c) Increased dry season rainfall in Can Tho using S-MK test. (d) Increased dry season rainfall in Can Tho using ITA. (e) Increased number of dry season rainfall days in Moc Hoa using S-MK test. (f) Increased number of dry season rainfall days in Moc Hoa using ITA.

Although annual rainfall in Moc Hoa decreased between 1978 and 2022, the change was not statistically significant. However, we found that the number of rain days increased

at the 95% confidence level. This increase occurred mainly during the dry season, with a 95% confidence level. On the contrary, rainfall in the wet season decreased at a 90% significance level because of a decrease in rainfall intensity. Aside from that, we discovered a drop in the number of days with rainfall that exceeded 50 mm, while the number of rainy days in the wet season remained unchanged. To understand how the pattern of rain changes over the rainy season, we investigated the pattern of rainfall in both Ca Mau and Moc Hoa. We considered both seasons in relation to Can Tho station. Figure 7 shows a 95% statistically significant decrease in rainfall volume for the month of August for Ca Mau.

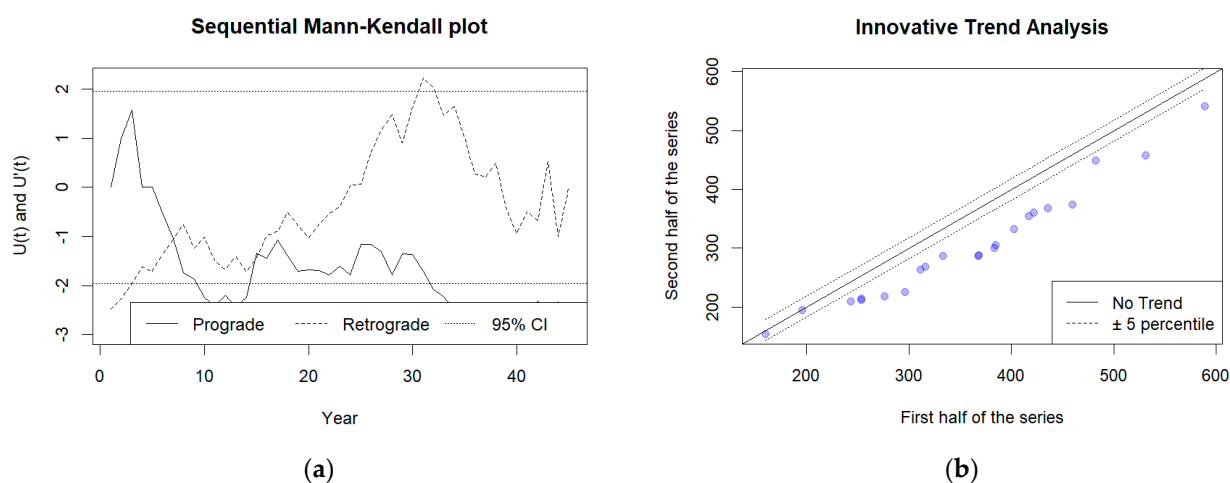


**Figure 7.** Decreased August rainfall at Ca Mau station using S-MK test (a) and ITA (b). (a) Decreased August rainfall at Ca Mau station using S-MK test. (b) Decreased August rainfall at Ca Mau station using ITA.

**Ca Mau station:** In general, August rainfall decreased with a statistical significance of 95%. In particular, the rainfall in the month of August has decreased significantly since 1986 and has increased again thereafter. Since 1991, the rainfall in August has decreased, and the rainfall has decreased significantly again since 2007. Results from the IAT and S-MK show that the August rainfall decreased at “medium” levels during the period from 1978 to 1998 and at the “low” level after 1991.

**Can Tho station:** Rainfall in the dry season months increased, but this is insignificant. It should be noted that rainfall increased in January and February with a 95% confidence level, according to the Mann–Kendall test results. However, there was no trend in the S-MK test results. Consequently, additional monitoring time is needed over these two months to precisely estimate future changes in rainfall. Just for the month of April, we found evidence of an increasing trend at the 90% significance level, whereas June rainfall decreased at a 90% confidence level. There was no trend detected for the months of March, July, October, or November. Monthly rainfall tended to decrease in the majority of wet season months at Can Tho station (June to October). Only August showed a reduction in rainfall at the 95% confidence level (Figure 8). It should be mentioned that the early rainy season months (i.e., June) also declined, but only by 90%. This should be considered when observing fluctuations in rainfall patterns in Can Tho.

At Moc Hoa station, the number of dry season months declined, although not significantly at the 95% confidence level. Remarkably, the rainfall only declined in May at the 90% significance level. Comparing Moc Hoa to the Ca Mau and Can Tho stations, there has been minimal variation in rainfall for the assessment period from 1978 to 2022.

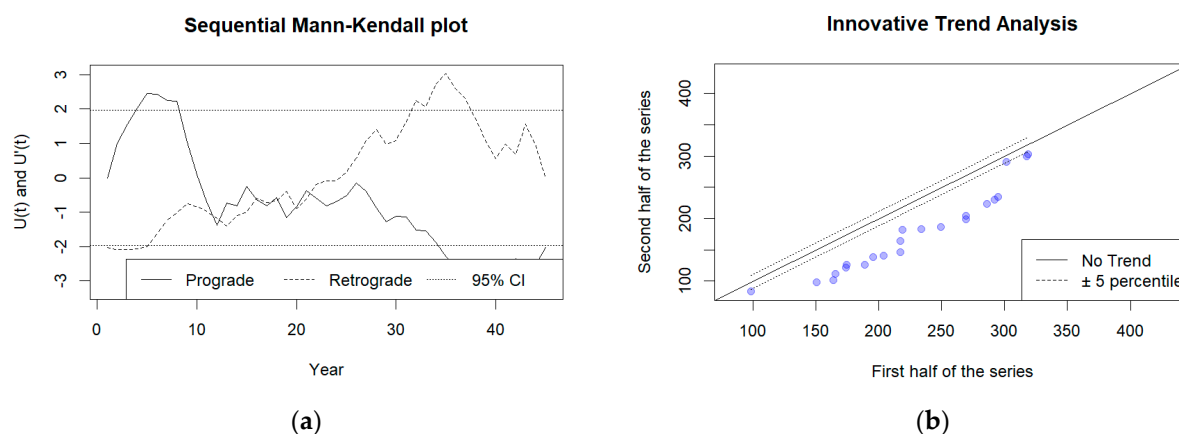


**Figure 8.** Decreased August rainfall in Can Tho station using the S-MK test (a) and ITA (b). (a) Decreased August rainfall in Can Tho using S-MK test. (b) Decreased August rainfall in Can Tho using ITA.

#### 4. Discussion

By analyzing how local climatic factors influence rainfall distribution, the findings from this study highlight the significant spatiotemporal variability in rainfall across the three selected meteorological stations in the VMD. The distinct seasonal rainfall distribution [62], which is characterized by significant differences between the coastal and inland stations [63], highlights the spatial heterogeneity [64], which is significantly associated with monsoon's role in shaping local climate patterns [65]. Specifically, the significant changes observed in seasonal rainfall (such as the decreased August rainfall at Ca Mau and the increased dry season rainfall at Can Tho) align with the known impacts of monsoonal shifts and changes in ENSO phases [66]. Further, the maximum daily rainfall and the number of days with rainfall exceeding 50 mm describing the variations in the intensity and frequency of rainfall events are evidence of the role of monsoon dynamics in the region [67]. The variability observed in our study, particularly the effects of El Niño and La Niña events, depicts broader global climate variability and its manifestation at local scales. The ENSO phenomenon plays a pivotal role in modulating global climate patterns, including the monsoon system in the VMD [68]. Our results show a clear correlation between ENSO events and rainfall variability, with La Niña years associated with higher rainfall and El Niño years associated with reduced rainfall [69]. By examining these correlations, our study provides insights on the local impacts of global climatic oscillations, as well as contributes to the understanding of how monsoon regions globally might respond to climate change.

Our study's findings on the annual and seasonal rainfall distributions across three meteorological stations in the VMD align with broader observations of hydroclimatic variability observed across the Mekong River Basin (MRB) [70]. The observed rainfall patterns, which are characterized by significant spatial variability and a notable influence of monsoon dynamics, are consistent with the complex hydrological regime that governs the MRB [71,72]. Comparative analyses with regional studies, such as those conducted by the Mekong River Commission (MRC) and various scientific and policy-oriented studies, reveal a consistent description of changing hydrological conditions across the MRB [73–75]. These changes are attributed to both natural climatic fluctuations, including the impact of El Niño and La Niña phenomena [76], and anthropogenic factors, such as upstream dam construction [77,78] and water resource management practices [79]. Hence, our study's observation of changed rainfall distributions and intensities can be interpreted as part of the broader hydrological shifts reported across the basin, which have significant implications for water security [80], agricultural productivity [81], and ecosystem health [82] in the VMD.

Furthermore, our analysis aligns with findings from studies highlighting the adverse impacts of climate change and human activities on the MRB's flow regimes. The joint

efforts by the MRC and other regional bodies to address these challenges through data sharing [83] and collaborative research initiatives [84] provide a critical context for interpreting our study's results. Specifically, as discussed above, the correlation between rainfall patterns in the VMD and broader hydrological changes underscores the interconnectedness of local and regional climate systems. The hydrological shifts due to climate change have been responsible for the heightened frequency of floods and the corresponding economic damage in the region [85]. Recent analyses have underscored the recurrent nature of floods in the VMD and the significant economic losses attributed to them [86]. Specifically, floods, which are driven by sea level rise and increased precipitation during the wet season, pose substantial economic challenges, highlighting the necessity for reliable loss and risk assessments [87–89]. In Can Tho City, for instance, floods have demonstrated that inundation duration significantly impacts the economy, with residential buildings and their contents being considerably affected [90]. This highlights the need for effective flood risk management strategies that account for the unique flooding characteristics of the VMD, where households have adapted to long inundation durations and shallow water depths [91]. Moreover, studies have emphasized the acute vulnerability of the VMD to coastal flooding, which is exacerbated by high tides and heavy rainfall [85,92]. A noteworthy event detailed the inundation of streets in Can Tho City to a depth of 50 cm, damaging 91 hectares of crops. This event serves as a potent reminder of the region's perennial risk of flooding [93]. Furthermore, the 2011 flood event in the Mekong Delta was among the most severe in recent history, resulting in 265 fatalities, damage to at least 449,000 houses, and an estimated economic loss of USD \$600 million [93]. These figures highlight the profound impact of flooding on the region, necessitating comprehensive strategies to mitigate future risks [94]. Hence, these findings, which illustrate the variability in rainfall patterns across the VMD, offer crucial insights for policymakers, environmental planners, and local communities. By understanding the dynamics of rainfall distribution and its implications on flood frequency and severity, targeted interventions can be developed to enhance flood preparedness and response strategies [95–102]. This is particularly relevant given the observed economic impacts of flooding events, which highlight the urgent need for improved flood loss modeling and risk assessments in the region [102].

Besides flooding, the variability in rainfall distribution and trends identified in our study also reflects the concerns raised by experts regarding water security in the VMD. The reported decrease in silt, sand, and nutrients [103,104], alongside the increasing incidents of saline intrusion [105] and coastal erosion [106], emphasizes the pressing need for a comprehensive strategy to ensure water security and sustainable development in the region. These findings call for enhanced cooperation among riparian countries, informed by accurate and timely hydrological data [107,108], to mitigate the adverse effects of climate variability and anthropogenic pressures on the MRB's hydrology. Hence, our study contributes to the growing body of evidence highlighting the significant impact of monsoon variability, climate change, and human activities on the hydrological dynamics of the VMD and the larger MRB. By providing detailed insights into rainfall patterns in the VMD, our research underscores the importance of region-specific studies in understanding the broader implications of hydroclimatic changes. Future research needs to focus on integrating local observations with regional climate models to improve predictions and inform water management strategies that can address the challenges posed by climate change and sustainable development in the MRB.

## 5. Conclusions

This study has provided a comprehensive analysis of rainfall distribution patterns across the Vietnamese Mekong Delta (VMD) over a 48-year period, uncovering significant spatial and temporal variability. Our investigation revealed a declining trend in total annual rainfall, with coastal regions, particularly Ca Mau, experiencing higher annual rainfall volumes compared with inland areas such as Can Tho and Moc Hoa. This spatial variability underscores the coastal environment's significant influence on rainfall distribution within

the VMD. Moreover, our analysis detected a significant decrease in annual and wet season rainfall in Ca Mau, alongside a marked reduction in rainfall during specific months like August and June, highlighting the potential impact of regional climatic factors, including the monsoon system. This study's findings also point to the nuanced effects of global climate phenomena such as El Niño and La Niña on the region's hydrology, which is evidenced by contrasting trends in wet and dry season rainfall volumes. Notably, an increase in dry season rainfall volumes, particularly in inland areas, suggests a shifting climatic pattern, which is potentially influenced by the aforementioned global phenomena. This shift has significant implications for water resource management, agricultural planning, and flood risk mitigation in the VMD. While the analysis presented in this study offers valuable insights into rainfall trends and their implications for the VMD, it is acknowledged that the scope was limited to data from three meteorological stations. This limitation, coupled with the exclusion of other climatic factors such as temperature, humidity, and wind patterns, suggests the need for a more holistic approach in future research. Investigating the interplay between rainfall and other climatic variables, alongside their socioeconomic impacts, could provide a more comprehensive understanding of the region's climatic dynamics. In light of these findings, it is imperative for policymakers and stakeholders to consider the complex interplay of local, regional, and global climatic factors in their efforts to adapt to and mitigate the impacts of changing rainfall patterns in the VMD. The role of monsoons, the influence of El Niño and La Niña events, and the recurrent challenge of floods necessitate a strategic approach to water resource management and disaster preparedness. Future research should aim to incorporate predictive models to forecast climatic changes and their potential impacts, thereby enabling more effective planning and adaptation strategies for the region. Hence, this study not only highlights the critical need for enhanced climatic monitoring and analysis in the VMD but also calls for an integrated approach to understanding and managing the complex climatic and hydrological challenges facing the region.

**Author Contributions:** Conceptualization, H.V.T.M., T.V.T., B.T.B.L., N.K.D., G.M. and P.K.; methodology, H.V.T.M., T.V.T., B.T.B.L., D.T.H.N., N.K.D., G.M. and P.K.; writing—original draft preparation, H.V.T.M., B.T.B.L., D.T.H.N., N.K.D., P.K., N.V.C.N. and N.P.C.; writing—review and editing, H.V.T.M., N.K.D., G.M. and P.K. All authors have read and agreed to the published version of the manuscript.

**Funding:** This research received no external funding.

**Institutional Review Board Statement:** Not applicable.

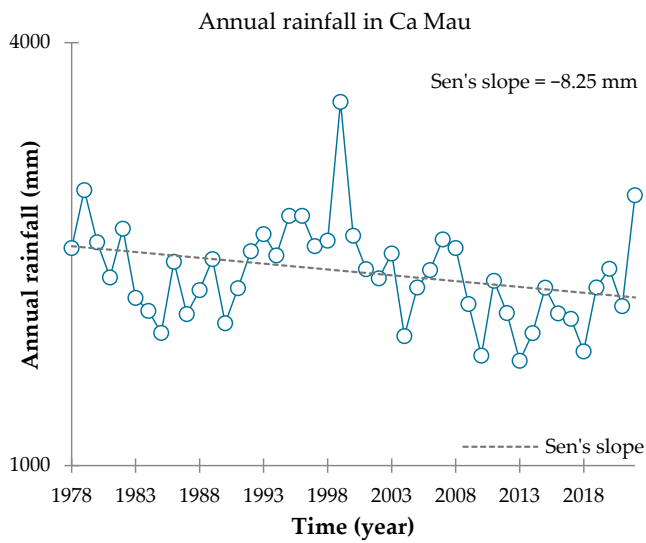
**Informed Consent Statement:** Not applicable.

**Data Availability Statement:** The data presented in this study are available on request from the corresponding author. The data not presented in this manuscript are not publicly available because it's being used for different internal purposes in Vietnam.

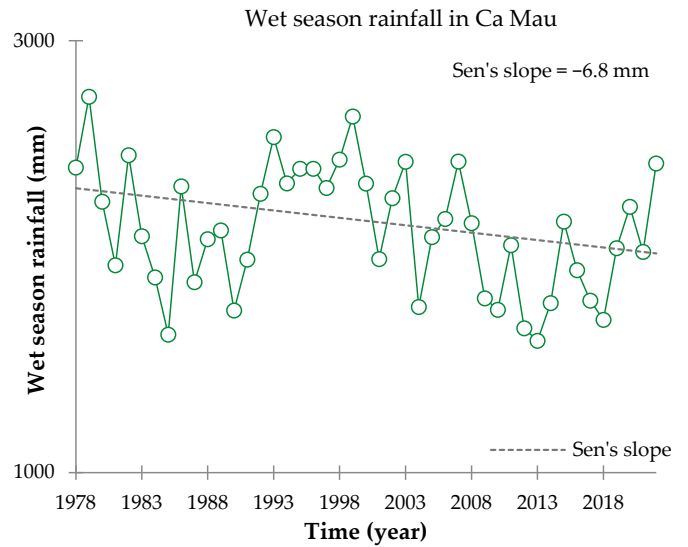
**Acknowledgments:** The authors acknowledge the help and support of the four anonymous reviewers whose critical comments helped us to improve our manuscript.

**Conflicts of Interest:** The authors declare no conflicts of interest.

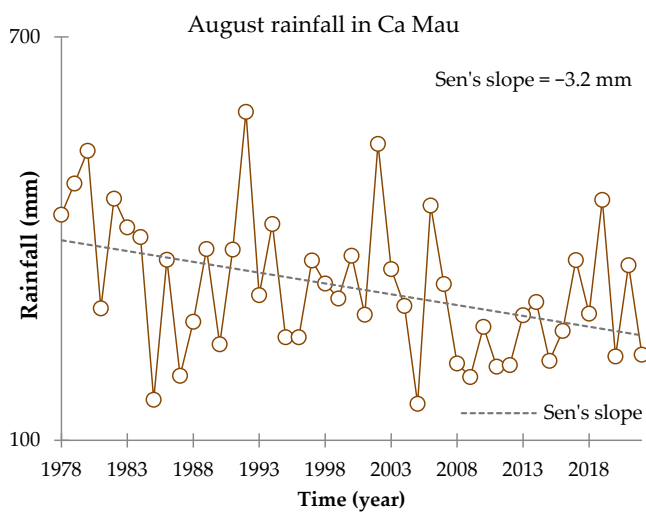
Appendix A



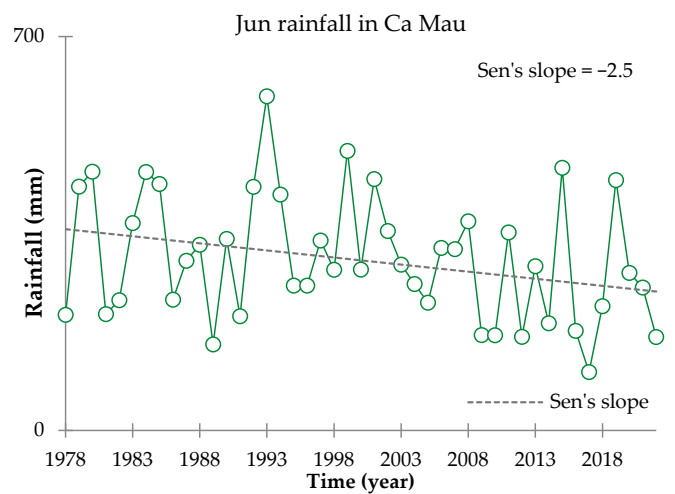
(a)



(b)



(c)



(d)

**Figure A1.** Rainfall trend patterns in Ca Mau station using Mann-Kendall test: (a) Annual rainfall decreasing trend in Ca Mau using Mann-Kendall test with a significance level of 95%. (b) Wet season rainfall decreasing trend in Ca Mau using Mann-Kendall test with a significance level of 90%. (c) Jun rainfall decreasing trend in Ca Mau using Mann-Kendall test with a significance level of 90%. (d) Jun rainfall decreasing trend in Ca Mau using Mann-Kendall test with a significance level of 90%.

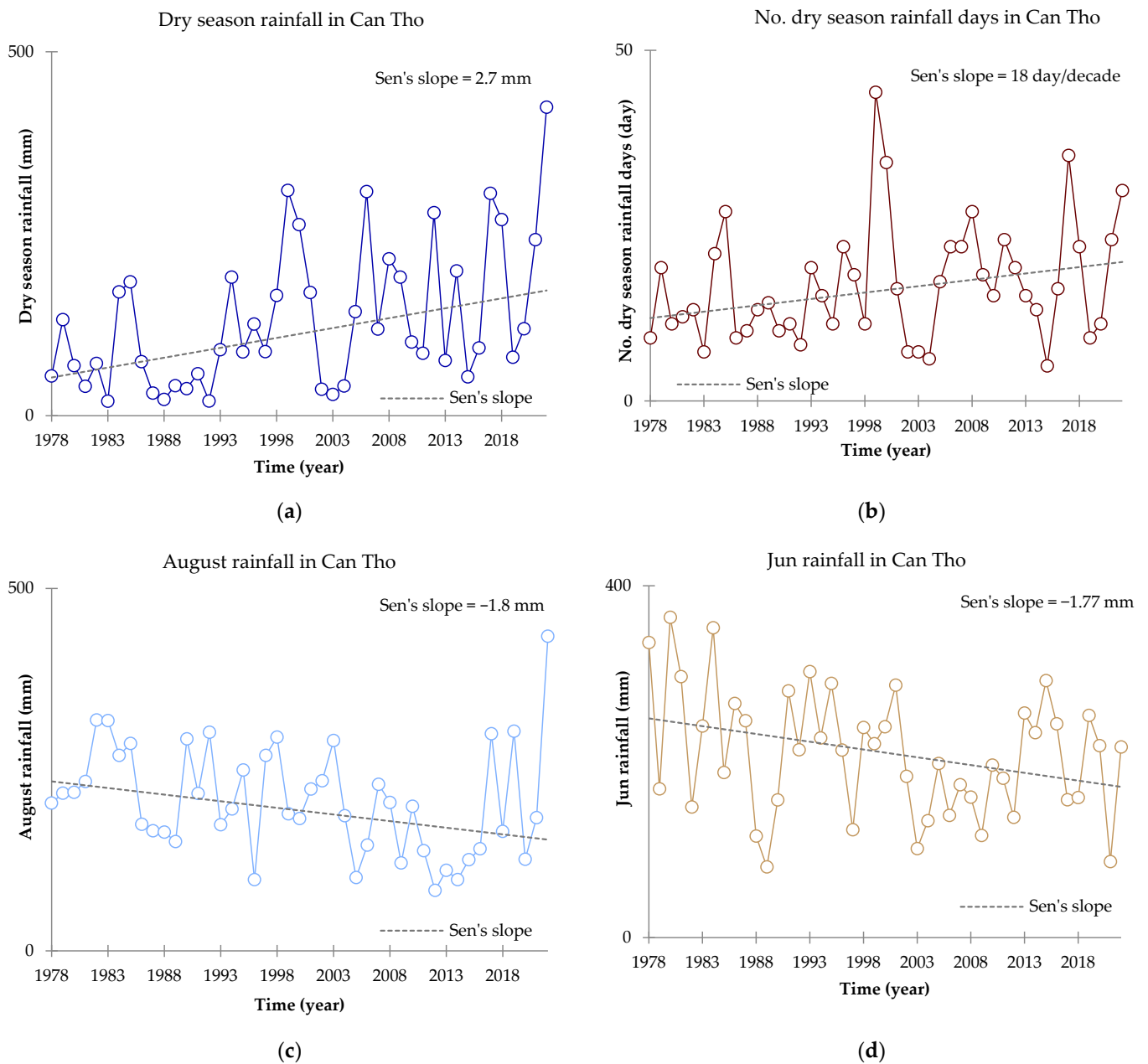


**Figure A2.** Rainfall trend patterns in Can Tho station using Mann-Kendall test: **(a)** Dry season rainfall day increasing trend in Can Tho using Mann-Kendall test with a significance level of 95%. **(b)** No. dry season rainfall day increasing trend in Can Tho using Mann-Kendall test with a significance level of 90%. **(c)** August rainfall decreasing trend in Can Tho using Mann-Kendall test with a significance level of 95%. **(d)** Jun rainfall decreasing trend in Can Tho using Mann-Kendall test with a significance level of 90%.

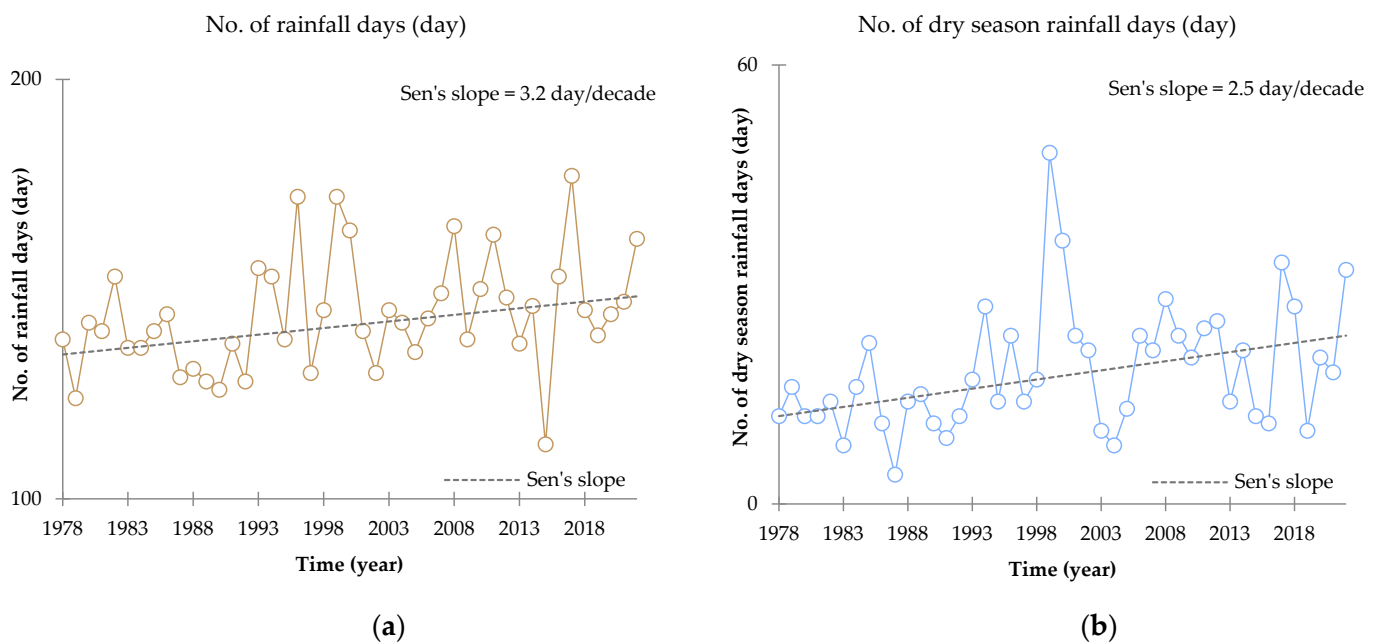


**Figure A3.** Rainfall trend patterns in Moc Hoa station using Mann-Kendall test: (a) Number of rainfall days increasing trend in Moc Hoa using Mann-Kendall test with a significance level of 95%. (b) Number of dry season rainfall days increasing trend in Moc Hoa using Mann-Kendall test with a significance level of 95%.

## References

- Juneng, L.; Tangang, F.T. Evolution of ENSO-Related Rainfall Anomalies in Southeast Asia Region and Its Relationship with Atmosphere–Ocean Variations in Indo-Pacific Sector. *Clim. Dyn.* **2005**, *25*, 337–350. [[CrossRef](#)]
- Chang, C.-P.; Wang, Z.; McBride, J.; Liu, C.-H. Annual Cycle of Southeast Asia—Maritime Continent Rainfall and the Asymmetric Monsoon Transition. *J. Clim.* **2005**, *18*, 287–301. [[CrossRef](#)]
- Li, X.-X. Heat Wave Trends in Southeast Asia during 1979–2018: The Impact of Humidity. *Sci. Total Environ.* **2020**, *721*, 137664. [[CrossRef](#)] [[PubMed](#)]
- Supari; Tangang, F.; Juneng, L.; Aldrian, E. Observed Changes in Extreme Temperature and Precipitation over Indonesia. *Int. J. Climatol.* **2017**, *37*, 1979–1997. [[CrossRef](#)]
- Yokoi, S.; Matsumoto, J. Collaborative Effects of Cold Surge and Tropical Depression–Type Disturbance on Heavy Rainfall in Central Vietnam. *Mon. Weather Rev.* **2008**, *136*, 3275–3287. [[CrossRef](#)]
- Gorin, V.A.; Scherz, M.D.; Korost, D.V.; Poyarkov, N.A. Consequences of Parallel Miniaturisation in Microhylinae (Anura, Microhylidae), with the Description of a New Genus of Diminutive South East Asian Frogs. *Zoosystematics Evol.* **2021**, *97*, 21–54. [[CrossRef](#)]
- Yang, S.; Li, Z.; Yu, J.Y.; Hu, X.; Dong, W.; He, S. El Niño–Southern Oscillation and its impact in the changing climate. *Natl. Sci. Rev.* **2018**, *5*, 840–857. [[CrossRef](#)]
- Minh, H.V.; Kumar, P.; Van Ty, T.; Duy, D.V.; Han, T.G.; Lavane, K.; Avtar, R. Understanding Dry and Wet Conditions in the Vietnamese Mekong Delta Using Multiple Drought Indices: A Case Study in Ca Mau Province. *Hydrology* **2022**, *9*, 213. [[CrossRef](#)]
- Cai, W.; McPhaden, M.J.; Grimm, A.M.; Rodrigues, R.R.; Taschetto, A.S.; Garreaud, R.D.; Dewitte, B.; Poveda, G.; Ham, Y.-G.; Santoso, A. Climate Impacts of the El Niño–Southern Oscillation on South America. *Nat. Rev. Earth Environ.* **2020**, *1*, 215–231. [[CrossRef](#)]
- Garcia, L. *Overview of Early Warning Systems for Hydro-Meteorological Hazards in Selected Countries in Southeast Asia*; Asian Disaster Preparedness Center: Bangkok, Thailand, 2002; p. 51.
- Nguyen-Thi, H.A.; Matsumoto, J.; Ngo-Duc, T.; Endo, N. A Climatological Study of Tropical Cyclone Rainfall in Vietnam. *Sola* **2012**, *8*, 41–44. [[CrossRef](#)]
- Anh, Q.T.; Taniguchi, K. Variations of Precipitation and Water Resources in the Northern Part of Vietnam under Climate Change. *J. Jpn. Soc. Civ. Eng. Ser. B1 (Hydraul. Eng.)* **2014**, *70*, I\_211–I\_216.
- Field, C.; Barros, V.; Dokken, D.; Mach, K.; Mastrandrea, M.; Bilir, T.; Chatterjee, M.; Ebi, K.; Estrada, Y.; Genova, R. *IPCC: Climate Change 2014: Impacts, Adaptation, and Vulnerability: Summaries, Frequently Asked Questions, and Cross-Chapter Boxes: A Working Group II Contribution to the Fifth Assessment Report of the Intergovernmental Panel on Climate Change*; World Meteorological Organization: Geneva, Switzerland, 2014; p. 705.

14. Thao, N.D.; Takagi, H.; Esteban, M. *Coastal Disasters and Climate Change in Vietnam: Engineering and Planning Perspectives*; Elsevier: Amsterdam, The Netherlands, 2014; ISBN 0-12-800479-7.
15. Sivakumar, B. Global Climate Change and Its Impacts on Water Resources Planning and Management: Assessment and Challenges. *Stoch. Environ. Res. Risk Assess.* **2011**, *25*, 583–600. [[CrossRef](#)]
16. DONRes, Vietnam. *Updated Climate Change Scenario 2020*; Ministry of Environment and Natural Resources: Ha Noi, Viet Nam, 2020; p. 254.
17. Das, S.; Kamruzzaman, M.; Islam, A.R.M.T. Assessment of characteristic changes of regional estimation of extreme rainfall under climate change: A case study in a tropical monsoon region with the climate projections from CMIP6 model. *J. Hydrol.* **2022**, *610*, 128002. [[CrossRef](#)]
18. Abdullah, A.Y.M.; Bhuian, M.H.; Kiselev, G.; Dewan, A.; Hassan, Q.K.; Rafiuddin, M. Extreme Temperature and Rainfall Events in Bangladesh: A Comparison between Coastal and Inland Areas. *Int. J. Climatol.* **2022**, *42*, 3253–3273. [[CrossRef](#)]
19. Xuan, N.V.; Giang, N.N.L.; Ty, T.V.; Kumar, P.; Downes, N.K.; Nam, N.D.G.; Ngan, N.V.C.; Thinh, L.V.; Duy, D.V.; Avtar, R. Impacts of Dike Systems on Hydrological Regime in Vietnamese Mekong Delta. *Water Supply* **2022**, *22*, 7945–7959. [[CrossRef](#)]
20. Kumar, V.; Jain, S.K.; Singh, Y. Analysis of Long-Term Rainfall Trends in India. *Hydrol. Sci. J.* **2010**, *55*, 484–496. [[CrossRef](#)]
21. Guo, A.; He, L. Correlations between Summer Discharge and South Asian Summer Monsoon Subsystems in Mekong River Basin. *Atmosphere* **2023**, *14*, 958. [[CrossRef](#)]
22. Tayyab, M.; Zhou, J.; Zeng, X.; Ahmed, I.; Adnan, R. *Application of Statistical Nonparametric Tests in Dongting Lake, China: 1961–2012*; IEEE: Piscataway, NJ, USA, 2016; pp. 197–201.
23. Da Silva, R.M.; Santos, C.A.; Moreira, M.; Corte-Real, J.; Silva, V.C.; Medeiros, I.C. Rainfall and River Flow Trends Using Mann–Kendall and Sen’s Slope Estimator Statistical Tests in the Cobres River Basin. *Nat. Hazards* **2015**, *77*, 1205–1221. [[CrossRef](#)]
24. Şen, Z. Innovative Trend Analysis Methodology. *J. Hydrol. Eng.* **2012**, *17*, 1042–1046. [[CrossRef](#)]
25. Bora, S.L.; Bhuyan, K.; Hazarika, P.J.; Gogoi, J.; Goswami, K. Analysis of Rainfall Trend Using Non-Parametric Methods and Innovative Trend Analysis during 1901–2020 in Seven States of North East India. *Curr. Sci.* **2022**, *122*, 801–811. [[CrossRef](#)]
26. Mallick, J.; Talukdar, S.; Alsubih, M.; Salam, R.; Ahmed, M.; Kahla, N.B.; Shamimuzzaman, M. Analysing the Trend of Rainfall in Asir Region of Saudi Arabia Using the Family of Mann-Kendall Tests, Innovative Trend Analysis, and Detrended Fluctuation Analysis. *Theor. Appl. Climatol.* **2021**, *143*, 823–841. [[CrossRef](#)]
27. Lavane, K.; Kumar, P.; Meraj, G.; Han, T.G.; Ngan, L.H.; Lien, B.T.; Van Ty, T.; Thanh, N.T.; Downes, N.K.; Nam, N.D.; et al. Assessing the Effects of Drought on Rice Yields in the Mekong Delta. *Climate* **2023**, *11*, 13. [[CrossRef](#)]
28. Minh, H.V.T.; Lavane, K.; Ty, T.V.; Downes, N.K.; Hong, T.T.K.; Kumar, P. Evaluation of the Impact of Drought and Saline Water Intrusion on Rice Yields in the Mekong Delta, Vietnam. *Water* **2022**, *14*, 3499. [[CrossRef](#)]
29. Agbo, E.P.; Nkajoe, U.; Edet, C.O. Comparison of Mann–Kendall and Şen’s Innovative Trend Method for Climatic Parameters over Nigeria’s Climatic Zones. *Clim. Dyn.* **2023**, *60*, 3385–3401. [[CrossRef](#)]
30. Serinaldi, F.; Chebana, F.; Kilsby, C.G. Dissecting Innovative Trend Analysis. *Stoch. Environ. Res. Risk Assess.* **2020**, *34*, 733–754. [[CrossRef](#)]
31. Myhre, G.; Alterskjær, K.; Stjern, C.W.; Hodnebrog, Ø.; Marelle, L.; Samset, B.H.; Sillmann, J.; Schaller, N.; Fischer, E.; Schulz, M.; et al. Frequency of Extreme Precipitation Increases Extensively with Event Rareness under Global Warming. *Sci. Rep.* **2019**, *9*, 16063. [[CrossRef](#)]
32. Minh, H.V.T.; Lavane, K.; Lanh, L.T.; Thinh, L.V.; Cong, N.P.; Ty, T.V.; Downes, N.K.; Kumar, P. Developing Intensity-Duration-Frequency (IDF) Curves Based on Rainfall Cumulative Distribution Frequency (CDF) for Can Tho City, Vietnam. *Earth* **2022**, *3*, 866–880. [[CrossRef](#)]
33. Tran, D.Q.; Nguyen, N.N.; Huynh, M.V.; Bairagi, S.K.; Le, K.N.; Tran, T.V.; Durand-Morat, A. Modeling Saltwater Intrusion Risk in the Presence of Uncertainty. *Sci. Total Environ.* **2024**, *908*, 168140. [[CrossRef](#)]
34. Evans, J.D. *Straightforward Statistics for the Behavioral Sciences*; Thomson Brooks/Cole Publishing Co.: Pacific Grove, CA, USA, 1996; ISBN 0-534-23100-4.
35. Tadić, L.; Bonacci, O.; Brleković, T. An Example of Principal Component Analysis Application on Climate Change Assessment. *Theor. Appl. Climatol.* **2019**, *138*, 1049–1062. [[CrossRef](#)]
36. Chan, J.C.; Shi, J. Application of Projection-pursuit Principal Component Analysis Method to Climate Studies. *Int. J. Climatol. J. R. Meteorol. Soc.* **1997**, *17*, 103–113. [[CrossRef](#)]
37. Zhang, J.; Chen, X.; Khan, A.; Zhang, Y.; Kuang, X.; Liang, X.; Taccari, M.L.; Nuttall, J. Daily Runoff Forecasting by Deep Recursive Neural Network. *J. Hydrol.* **2021**, *596*, 126067. [[CrossRef](#)]
38. Maćkiewicz, A.; Ratajczak, W. Principal Components Analysis (PCA). *Comput. Geosci.* **1993**, *19*, 303–342. [[CrossRef](#)]
39. Holland, S.M. *Principal Components Analysis (PCA)*; Department of Geology, University of Georgia: Athens, GA, USA, 2008; Volume 30602, p. 2501.
40. Kurita, T. Principal Component Analysis (PCA). In *Computer Vision: A Reference Guide*; Springer: New York, NY, USA, 2019; pp. 1–4.
41. Lornezhad, E.; Ebrahimi, H.; Rabieifar, H.R. Analysis of Precipitation and Drought Trends by a Modified Mann–Kendall Method: A Case Study of Lorestan Province, Iran. *Water Supply* **2023**, *23*, 1557–1570. [[CrossRef](#)]
42. Tosunoğlu, F. Trend Analysis of Daily Maximum Rainfall Series in Çoruh Basin, Turkey. *J. Inst. Sci. Technol.* **2017**, *7*, 195–205. [[CrossRef](#)]

43. Hanif, M.F.; Mustafa, M.R.U.; Liaqat, M.U.; Hashim, A.M.; Yusof, K.W. Evaluation of Long-Term Trends of Rainfall in Perak, Malaysia. *Climate* **2022**, *10*, 44. [[CrossRef](#)]
44. Kisi, O.; Ay, M. Comparison of Mann–Kendall and Innovative Trend Method for Water Quality Parameters of the Kizilirmak River, Turkey. *J. Hydrol.* **2014**, *513*, 362–375. [[CrossRef](#)]
45. Kendall, M. *Rank Correlation Methods*, 4th ed.; Charles Griffin: London, UK, 1975.
46. Mann, H.B. Nonparametric Tests against Trend. *Econom. J. Econom. Soc.* **1945**, *13*, 245–259.
47. Sen, P.K. Estimates of the Regression Coefficient Based on Kendall’s Tau. *J. Am. Stat. Assoc.* **1968**, *63*, 1379–1389. [[CrossRef](#)]
48. Gilbert, R.O. *Statistical Methods for Environmental Pollution Monitoring*; John Wiley & Sons: Hoboken, NJ, USA, 1987; ISBN 0-471-28878-0.
49. Zeybekoğlu, U. Temperature Series Analysis of the Hirfanli Dam Basin with the Mann-Kendall and Sequential Mann-Kendall Tests. *Turk. J. Eng.* **2023**, *7*, 306–313. [[CrossRef](#)]
50. Şen, Z. Trend Identification Simulation and Application. *J. Hydrol. Eng.* **2014**, *19*, 635–642. [[CrossRef](#)]
51. Caloiero, T.; Coscarelli, R.; Ferrari, E. Application of the Innovative Trend Analysis Method for the Trend Analysis of Rainfall Anomalies in Southern Italy. *Water Resour. Manag.* **2018**, *32*, 4971–4983. [[CrossRef](#)]
52. Alifujiang, Y.; Abuduwaili, J.; Maihemuti, B.; Emin, B.; Groll, M. Innovative Trend Analysis of Precipitation in the Lake Issyk-Kul Basin, Kyrgyzstan. *Atmosphere* **2020**, *11*, 332. [[CrossRef](#)]
53. Alashan, S. An Improved Version of Innovative Trend Analyses. *Arab. J. Geosci.* **2018**, *11*, 50. [[CrossRef](#)]
54. Suhaila, J.; Deni, S.M.; Wan Zin, W.Z.; Jemain, A.A. Spatial patterns and trends of daily rainfall regime in Peninsular Malaysia during the southwest and northeast monsoons: 1975–2004. *Meteorol. Atmos. Phys.* **2010**, *110*, 1–18. [[CrossRef](#)]
55. Dunn, C.H. *Base Development in South Vietnam, 1965–1970*; Department of the Army: Monterey, CA, USA, 1973.
56. Qian, W.; Ding, T.; Hu, H.; Lin, X.; Qin, A. An overview of dry-wet climate variability among monsoon-westerly regions and the monsoon northernmost marginal active zone in China. *Adv. Atmos. Sci.* **2009**, *26*, 630–641. [[CrossRef](#)]
57. Chen, L.; Dong, M.; Shao, Y. The characteristics of interannual variations on the East Asian monsoon. *J. Meteorol. Soc. Jpn. Ser. II* **1992**, *70*, 397–421. [[CrossRef](#)]
58. Ke, M.; Wang, Z.; Pan, W.; Luo, H.; Yang, S.; Guo, R. Extremely Strong Western Pacific Subtropical High in May 2021 Following a La Niña Event: Role of the Persistent Convective Forcing over the Indian Ocean. *Asia-Pac. J. Atmos. Sci.* **2023**, *59*, 47–58. [[CrossRef](#)]
59. Freund, M.B.; Henley, B.J.; Karoly, D.J.; McGregor, H.V.; Abram, N.J.; Dommenges, D. Higher frequency of Central Pacific El Niño events in recent decades relative to past centuries. *Nat. Geosci.* **2019**, *12*, 450–455. [[CrossRef](#)]
60. Soman, M.K.; Kumar, K.K. Some aspects of daily rainfall distribution over India during the south-west monsoon season. *Int. J. Climatol.* **1990**, *10*, 299–311. [[CrossRef](#)]
61. Wang, B.; Li, J.; He, Q. Variable and robust East Asian monsoon rainfall response to El Niño over the past 60 years (1957–2016). *Adv. Atmos. Sci.* **2017**, *34*, 1235–1248. [[CrossRef](#)]
62. Miralles, D.G.; Van Den Berg, M.J.; Gash, J.H.; Parinussa, R.M.; De Jeu, R.A.; Beck, H.E.; Holmes, T.R.; Jiménez, C.; Verhoest, N.E.; Dorigo, W.A.; et al. El Niño–La Niña cycle and recent trends in continental evaporation. *Nat. Clim. Chang.* **2014**, *4*, 122–126. [[CrossRef](#)]
63. Qian, W.; Kang, H.S.; Lee, D.K. Distribution of seasonal rainfall in the East Asian monsoon region. *Theor. Appl. Climatol.* **2002**, *73*, 151–168. [[CrossRef](#)]
64. Chen, G.; Lan, R.; Zeng, W.; Pan, H.; Li, W. Diurnal variations of rainfall in surface and satellite observations at the monsoon coast (South China). *J. Clim.* **2018**, *31*, 1703–1724. [[CrossRef](#)]
65. Ghosh, S.; Vittal, H.; Sharma, T.; Karmakar, S.; Kasiviswanathan, K.S.; Dhanesh, Y.; Sudheer, K.P.; Gunthe, S.S. Indian summer monsoon rainfall: Implications of contrasting trends in the spatial variability of means and extremes. *PLoS ONE* **2016**, *11*, e0158670. [[CrossRef](#)]
66. Paul, S.; Ghosh, S.; Mathew, M.; Devanand, A.; Karmakar, S.; Niyogi, D. Increased spatial variability and intensification of extreme monsoon rainfall due to urbanization. *Sci. Rep.* **2018**, *8*, 3918. [[CrossRef](#)]
67. Gill, E.C.; Rajagopalan, B.; Molnar, P. Subseasonal variations in spatial signatures of ENSO on the Indian summer monsoon from 1901 to 2009. *J. Geophys. Res. Atmos.* **2015**, *120*, 8165–8185. [[CrossRef](#)]
68. May, W. Simulation of the variability and extremes of daily rainfall during the Indian summer monsoon for present and future times in a global time-slice experiment. *Clim. Dyn.* **2004**, *22*, 183–204. [[CrossRef](#)]
69. Le, P.V.; Pham, H.V.; Bui, L.K.; Tran, A.N.; Pham, C.V.; Nguyen, G.V.; Tran, P.A. Responses of groundwater to precipitation variability and ENSO in the Vietnamese Mekong Delta. *Hydrol. Res.* **2021**, *52*, 1280–1293. [[CrossRef](#)]
70. Kripalani, R.H.; Kulkarni, A. Rainfall variability over South-east Asia—Connections with Indian monsoon and ENSO extremes: New perspectives. *Int. J. Climatol. J. R. Meteorol. Soc.* **1997**, *17*, 1155–1168. [[CrossRef](#)]
71. Van Binh, D.; Kantoush, S.A.; Saber, M.; Mai, N.P.; Maskey, S.; Phong, D.T.; Sumi, T. Long-term alterations of flow regimes of the Mekong River and adaptation strategies for the Vietnamese Mekong Delta. *J. Hydrol. Reg. Stud.* **2020**, *32*, 100742. [[CrossRef](#)]
72. Sun, Z.; Liu, Y.; Zhang, J.; Chen, H.; Jin, J.; Liu, C.; Wang, G.; Tang, L. Spatiotemporal Projections of Precipitation in the Lancang–Mekong River Basin Based on CMIP6 Models. *Remote Sens.* **2023**, *15*, 4502. [[CrossRef](#)]
73. Tri, V.P.D.; Yarina, L.; Nguyen, H.Q.; Downes, N.K. Progress toward Resilient and Sustainable Water Management in the Vietnamese Mekong Delta. *WIREs Water* **2023**, *10*, e1670. [[CrossRef](#)]

74. Khoi, D.N.; Nguyen, V.T.; Sam, T.T.; Ky Phung, N.; Thi Bay, N. Responses of river discharge and sediment load to climate change in the transboundary Mekong River Basin. *Water Environ. J.* **2020**, *34*, 367–380. [CrossRef]
75. Rossi, C.G.; Srinivasan, R.; Jirayoot, K.; Le Duc, T.; Souvannabouth, P.; Binh, N.; Gassman, P.W. Hydrologic evaluation of the Lower Mekong River Basin with the soil and water assessment tool model. *Int. Agric. Eng. J.* **2009**, *18*, 1–13.
76. Wang, C.; Leisz, S.; Li, L.; Shi, X.; Mao, J.; Zheng, Y.; Chen, A. Historical and projected future runoff over the Mekong River basin. *Earth Syst. Dyn.* **2024**, *15*, 75–90. [CrossRef]
77. Räsänen, T.A.; Kumm, M. Spatiotemporal influences of ENSO on precipitation and flood pulse in the Mekong River Basin. *J. Hydrol.* **2013**, *476*, 154–168. [CrossRef]
78. Sridhar, V.; Kang, H.; Ali, S.A. Human-induced alterations to land use and climate and their responses for hydrology and water management in the Mekong River Basin. *Water* **2019**, *11*, 1307. [CrossRef]
79. Yang, J.; Yang, Y.E.; Chang, J.; Zhang, J.; Yao, J. Impact of dam development and climate change on hydroecological conditions and natural hazard risk in the Mekong River Basin. *J. Hydrol.* **2019**, *579*, 124177. [CrossRef]
80. Piman, T.; Lennaerts, T.; Southalack, P. Assessment of hydrological changes in the lower Mekong Basin from Basin-Wide development scenarios. *Hydrol. Process.* **2013**, *27*, 2115–2125. [CrossRef]
81. Liu, J.; Chen, D.; Mao, G.; Irannezhad, M.; Pokhrel, Y. Past and future changes in climate and water resources in the Lancang–Mekong River Basin: Current understanding and future research directions. *Engineering* **2022**, *13*, 144–152. [CrossRef]
82. Pokhrel, Y.; Burbano, M.; Roush, J.; Kang, H.; Sridhar, V.; Hyndman, D.W. A review of the integrated effects of changing climate, land use, and dams on Mekong river hydrology. *Water* **2018**, *10*, 266. [CrossRef]
83. Li, D.; Long, D.; Zhao, J.; Lu, H.; Hong, Y. Observed changes in flow regimes in the Mekong River basin. *J. Hydrol.* **2017**, *551*, 217–232. [CrossRef]
84. Thu, H.N.; Wehn, U. Data sharing in international transboundary contexts: The Vietnamese perspective on data sharing in the Lower Mekong Basin. *J. Hydrol.* **2016**, *536*, 351–364. [CrossRef]
85. Heikkilä, T.; Gerlak, A.K.; Bell, A.R.; Schmeier, S. Adaptation in a transboundary river basin: Linking stressors and adaptive capacity within the Mekong River Commission. *Environ. Sci. Policy* **2013**, *25*, 73–82. [CrossRef]
86. Triet, N.V.K.; Dung, N.V.; Hoang, L.P.; Le Duy, N.; Tran, D.D.; Anh, T.T.; Kumm, M.; Merz, B.; Apel, H. Future projections of flood dynamics in the Vietnamese Mekong Delta. *Sci. Total Environ.* **2020**, *742*, 140596. [CrossRef] [PubMed]
87. Balica, S.F.; Dinh, Q.; Popescu, I. Vulnerability and exposure in developed and developing countries: Large-scale assessments. In *Hydro-Meteorological Hazards, Risks, and Disasters*; Elsevier: Amsterdam, The Netherlands, 2023; pp. 103–143.
88. Chinh, D.T.; Bubeck, P.; Dung, N.V.; Kreibich, H. The 2011 flood event in the Mekong Delta: Preparedness, response, damage and recovery of private households and small businesses. *Disasters* **2016**, *40*, 753–778. [CrossRef] [PubMed]
89. Wassmann, R.; Hien, N.X.; Hoanh, C.T.; Tuong, T.P. Sea level rise affecting the Vietnamese Mekong Delta: Water elevation in the flood season and implications for rice production. *Clim. Chang.* **2004**, *66*, 89–107. [CrossRef]
90. Triet, N.V.K.; Dung, N.V.; Merz, B.; Apel, H. Towards risk-based flood management in highly productive paddy rice cultivation—concept development and application to the Mekong Delta. *Nat. Hazards Earth Syst. Sci.* **2018**, *18*, 2859–2876. [CrossRef]
91. Chinh, D.T.; Dung, N.V.; Gain, A.K.; Kreibich, H. Flood loss models and risk analysis for private households in Can Tho City, Vietnam. *Water* **2017**, *9*, 13. [CrossRef]
92. Chinh, D.T.; Gain, A.K.; Dung, N.V.; Haase, D.; Kreibich, H. Multi-variate analyses of flood loss in Can Tho City, Mekong Delta. *Water* **2015**, *8*, 6. [CrossRef]
93. Van Tho, N. Coastal erosion, river bank erosion and landslides in the Mekong Delta: Causes, effects and solutions. In *Geotechnics for Sustainable Infrastructure Development*; Springer: Singapore, 2020; pp. 957–962.
94. Mekong Floods Are a Reminder of a Perennial Risk. JBA Risk Management. Mekong Delta Flood Report. Available online: <https://www.jbarisk.com/products-services/event-response/mekong-delta-flood-report/> (accessed on 4 February 2024).
95. MRC. *Annual Mekong Flood Report 2015*; Mekong River Commission: Vientiane, Laos, 2018; 106p.
96. Bhattarai, R.; Mishra, B.K.; Bhattarai, D.; Khatiwada, D.; Kumar, P.; Meraj, G. Assessing Hydropower Potential in Nepal’s Sunkoshi River Basin: An Integrated GIS and SWAT Hydrological Modeling Approach. *Scientifica* **2024**, *2024*, 1007081. [CrossRef]
97. Dolgorsuren, S.E.; Ishgaldan, B.; Myagmartseren, P.; Kumar, P.; Meraj, G.; Singh, S.K.; Kanga, S.; Almazroui, M. Hydrological Responses to Climate Change and Land-Use Dynamics in Central Asia’s Semi-arid Regions: An SWAT Model Analysis of the Tuul River Basin. *Earth Syst. Environ.* **2024**. [CrossRef]
98. Debnath, J.; Debnath, A.; Meraj, G.; Chand, K.; Singh, S.K.; Kanga, S.; Kumar, P.; Sahariah, D.; Saikia, A. Flood susceptibility assessment of the Agartala Urban Watershed, India, using Machine Learning Algorithm. *Environ. Monit. Assess.* **2024**, *196*, 110. [CrossRef]
99. Debnath, J.; Sahariah, D.; Nath, N.; Saikia, A.; Lahon, D.; Islam, M.N.; Hashimoto, S.; Meraj, G.; Kumar, P.; Singh, S.K.; et al. Modelling on assessment of flood risk susceptibility at the Jia Bharali River basin in Eastern Himalayas by integrating multicollinearity tests and geospatial techniques. *Model. Earth Syst. Environ.* **2023**. [CrossRef]
100. Debnath, J.; Sahariah, D.; Lahon, D.; Nath, N.; Chand, K.; Meraj, G.; Kumar, P.; Singh, S.K.; Kanga, S.; Farooq, M. Assessing the impacts of current and future changes of the planforms of river Brahmaputra on its land use-land cover. *Geosci. Front.* **2023**, *14*, 101557. [CrossRef]

101. Rafiq, M.; Meraj, G.; Kesarkar, A.P.; Farooq, M.; Singh, S.K.; Kanga, S. Hazard mitigation and climate change in the Himalayas—policy and decision making. In *Disaster Management in the Complex Himalayan Terrains: Natural Hazard Management, Methodologies and Policy Implications*; Springer International Publishing: Cham, Switzerland, 2022; pp. 169–182.
102. Tomar, P.; Singh, S.K.; Kanga, S.; Meraj, G.; Kranjčić, N.; Đurin, B.; Pattanaik, A. GIS-Based Urban Flood Risk Assessment and Management—A Case Study of Delhi National Capital Territory (NCT), India. *Sustainability* **2021**, *13*, 12850. [[CrossRef](#)]
103. Dinh, Q.; Balica, S.; Popescu, I.; Jonoski, A. Climate change impact on flood hazard, vulnerability and risk of the Long Xuyen Quadrangle in the Mekong Delta. *Int. J. River Basin Manag.* **2012**, *10*, 103–120. [[CrossRef](#)]
104. Nhan, N.H.; Cao, N.B. Damming the Mekong: Impacts in Vietnam and solutions. In *Coasts and Estuaries*; Elsevier: Amsterdam, The Netherlands, 2019; pp. 321–340.
105. Hui, T.R.; Park, E.; Loc, H.H.; Tien, P.D. Long-term hydrological alterations and the agricultural landscapes in the Mekong Delta: Insights from remote sensing and national statistics. *Environ. Chall.* **2022**, *7*, 100454. [[CrossRef](#)]
106. Loc, H.H.; Van Binh, D.; Park, E.; Shrestha, S.; Dung, T.D.; Son, V.H.; Truc, N.H.T.; Mai, N.P.; Seijger, C. Intensifying saline water intrusion and drought in the Mekong Delta: From physical evidence to policy outlooks. *Sci. Total Environ.* **2021**, *757*, 143919. [[CrossRef](#)]
107. Feng, Y.; Wang, W.; Suman, D.; Yu, S.; He, D. Water cooperation priorities in the Lancang-Mekong River basin based on cooperative events since the Mekong River Commission establishment. *Chin. Geogr. Sci.* **2019**, *29*, 58–69. [[CrossRef](#)]
108. Schmeier, S. Regional cooperation efforts in the Mekong river basin: Mitigating river-related security threats and promoting regional development. *Austrian J. Southeast Asian Stud.* **2009**, *2*, 28–52.

**Disclaimer/Publisher’s Note:** The statements, opinions and data contained in all publications are solely those of the individual author(s) and contributor(s) and not of MDPI and/or the editor(s). MDPI and/or the editor(s) disclaim responsibility for any injury to people or property resulting from any ideas, methods, instructions or products referred to in the content.